Sgríbhinní Institiúid Árd-Léighinn
Bhaile Átha Cliath. Sraith A Uimh. 4
Communications of the Dublin Institute for
Advanced Studies. Series A No. 4

COSMIC RAYS

BY

L. JÁNOSSY

DUBLIN
THE DUBLIN INSTITUTE FOR ADVANCED STUDIES
64-5 MERRION SQUARE
1947

COSMIC RAYS.[1]

By L. JÁNOSSY,

Formerly at the University of Manchester.

I.—Introduction.

Cosmic rays at sea-level contain at least three different components. Two of the components, the hard component and the soft component, are well known and have been studied extensively. The hard component is of secondary origin and is due to a primary component, which may be called the third component. In Chapters II–IV we shall deal with the properties of this third component. As an introduction, however, we shall give a brief summary of the more important features of cosmic rays.

A. *Hard and soft components.*

The existence of at least two distinct components in the cosmic ray beam near sea-level and at moderate altitudes can be demonstrated by simple absorption experiments.

Consider a counter arrangement consisting of two counters in coincidence (fig. 1). The rate of coincidences plotted as a function of the

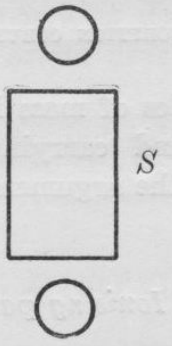

Fig. 1.—Coincidence arrangement.

thickness of absorber S placed between the counters gives the absorption curve of the radiation. A typical absorption curve is shown in fig. 2. It is seen that the coincidence rate is decreased by about 30 per cent due to the first 10 cm. of lead absorber, while the intensity drops to about half between 10 cm. and 1 m. of lead.

[1] Lectures delivered at the Dublin Institute for Advanced Studies, 1945.

The first rapid drop is due to the absorption of the soft component; it is the hard component which penetrates greater thicknesses.

Hard and soft components can also be identified by cloud chamber photographs. Figs. 3 and 4 show examples of a hard and of a soft particle traversing a lead plate placed across the cloud chamber. The hard particle traverses the plate without giving rise to any secondary effect and without being scattered appreciably. The soft particle seen to enter the lead plate in fig. 4 emerges together with a number of secondaries, giving rise to a small shower.

B. *The Nature of the hard and the soft components.*

It is now known that the soft component consists of positive and negative electrons together with photons. The hard component consists

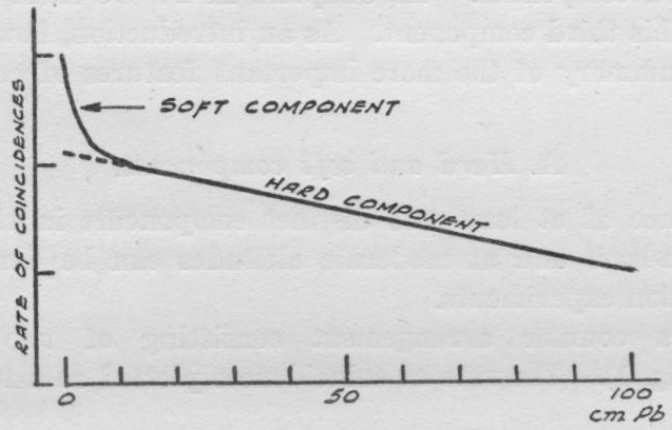

FIG. 2.—ABSORPTION CURVE (SCHEMATICAL).

of mesons—that is, of particles of mass intermediate between that of the electron and the proton, and carrying positive or negative electric charge. We now reproduce the arguments which led to the identification of the two components.

(a) *Ionising particles.*

The bulk of the cosmic ray particles are ionising, i.e. they are electrically charged. After the discovery of cosmic rays it was first wrongly assumed that they were non-ionising rays; the fact that the cosmic rays consist mainly of ionising particles was first realised by Bothe and Kolhörster (1929). It was found that cosmic rays passing through two counters will discharge them both. Non-ionising rays, e.g. photons, could only give coincident discharges as a result of the production of ionising secondaries in each counter; and the probability of the process would be very small.

Tracks of cosmic rays observed in a cloud chamber first by Skobelzyn (1927, 9) and then by many others showed directly that ionising particles were present.

The above experiments showed clearly that cosmic rays contain ionising particles. The question arose, however, whether these ionising particles formed the main cosmic ray beam or whether they were secondaries of a more penetrating non-ionising radiation.

Absorption experiments (Rossi, (1933), Street, Woodward and Stevenson (1935)) showed that about 50 per cent of the hard component consists of particles capable of penetrating more than 1 m. of lead. The energy loss in 1 m. of lead must be assumed to be comparable with that suffered by a particle traversing vertically the whole of the atmosphere. It is seen, therefore, that about half of the penetrating particles observed at sea-level have remaining ranges exceeding the equivalent of the atmosphere. The same conclusion could be drawn from the measurement of the momentum spectrum of the cosmic ray particles by means of a cloud chamber in a magnetic field. The measurements of Kunze (1933), Anderson and Neddermeyer (1937), Blackett (1937) and others showed that about half of the cosmic ray particles at sea-level have momenta exceeding 3000 MEV/c. It is estimated that the loss of energy of a singly charged particle due to ionisation when traversing the atmosphere is 2000 MEV (see below).

Thus many of the cosmic ray particles at sea-level have momenta which would be sufficient to traverse the atmosphere once more. It is seen, therefore, that, regarding merely their energy, the particles of the hard component might have come from outside the atmosphere. In actual fact, however, the penetrating particles do not come from outside the atmosphere, but they have their origin near the top of the atmosphere.

(b) *Charge and velocity.*

The rate of ionisation of a particle of charge Z velocity v and momentum p is proportional to

$$J \longrightarrow Z^2 (c/v)^2 f(p) \qquad \ldots . \quad (1)$$

where $f(p)$ is a function which increases logarithmically with increasing p. For not too large ranges of p the function $f(p)$ can be regarded as nearly constant (see fig. 5).

We note from (1) that the rate of ionisation of fast particles ($v \backsim c$) of single charges ($Z = 1$) has a value which is nearly independent of any other properties of the particle. In particular, the rate of ionisation of fast singly charged particles is nearly independent of their rest mass.

The ionisation density observed along the tracks of most cosmic ray particles is of the same order as that found for fast β-particles. Hence

it is concluded that most cosmic ray particles are singly charged and move with velocities near *c*.

The sign of charge of a cosmic ray particle can be determined from its curvature in a known magnetic field, provided the direction of motion of the particle is known. Most cosmic ray particles move downwards, and, therefore, for statistical purposes it is permissible to determine the sign of charge of particles crossing a chamber assuming that all move downwards. It is thus found that cosmic rays contain about equal numbers of positively and negatively charged particles with a slight excess of positively charged ones.

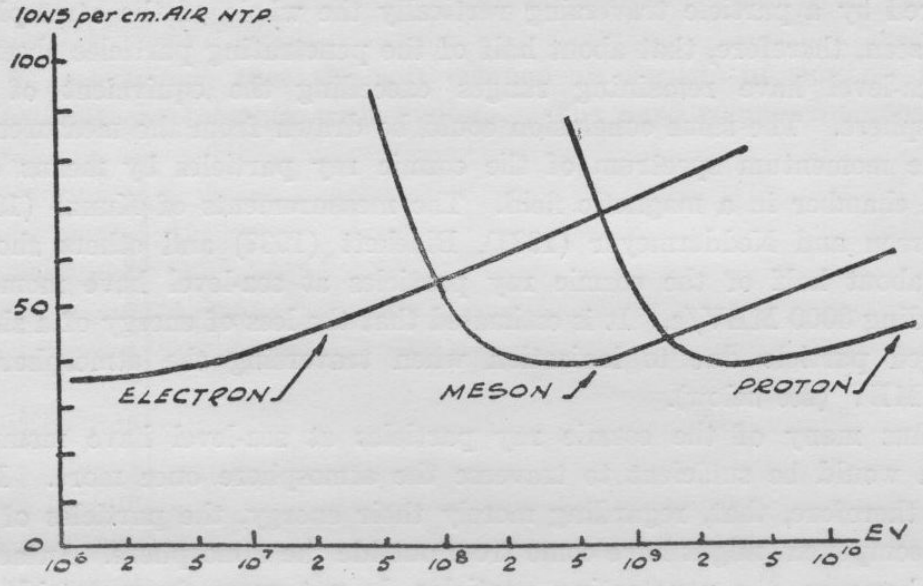

FIG. 5—IONISATION-ENERGY DIAGRAMS FOR ELECTRON, MESON AND PROTON.

(c) *Mass.*

(i) The density of ionisation along the track of a fast particle is nearly independent of the rest mass of the particle; therefore, fast tracks cannot be used for the determination of mass. The track of a fast particle deflected in a magnetic field can, however, be used to find an upper limit for the rest mass m_0 of the particle.

For a particle with velocity

$$v = c/\sqrt{2} \qquad \ldots\ (2)$$

we have

$$p = m_0 c \qquad \ldots\ (3)$$

According to (1), a particle of velocity $c/\sqrt{2}$ ionises about twice as much as a "fast" particle. Thus, if we find a track with an ionisation

density not exceeding twice that of a fast particle, we can conclude that the rest mass of the particle

$$m_0 \leqslant p/c \qquad \ldots\ldots (4)$$

We note, that fast particles of a few MEV/c momentum cannot be much heavier than electrons; such particles observed among cosmic rays are assumed to be electrons.

A track with ionisation twice the minimum density will appear slightly denser than the track of a fast particle. Under usual experimental conditions, it is not safe to classify a particle as slow unless its density of ionisation is three to four times the minimum density.

Investigation of electron tracks by Anderson (1932, 3) and later by Blackett and Occhialini (1933) led to the discovery of the positive electron.

The equation (4) gives no useful information for particles with momentum exceeding, say, 1000 MEV/c. It was stressed, however, by Williams (1934) that electrons with momentum exceeding 1000 MEV/c ought to ionise noticeably more than ordinary β-particles because of the increase in the function $f(p)$ with momentum. As the density of ionisation of cosmic ray particles does not seem to change between a few MEV/c and 1000 MEV/c, Williams concluded that the particles with high momentum are not electrons, but particles of greater mass.

(ii) It can be concluded from the observed penetrating power of cosmic ray particles, that most of the particles are not electrons but particles of greater mass.

Electrons of energy exceeding 10 $m_e c^2$ lose a large amount of energy by radiative collisions. The cross-section for radiation loss increases with the primary energy, and, therefore, the range of energetic electrons is severely limited by this process. The average free path of an energetic electron is about 0·5 cm. of lead or 40 cm. of water.

The particles of the soft component of cosmic rays lose energies in accordance with the prediction of theory, as was shown by Anderson and Neddermeyer (1934), Blackett and Wilson (1937) and others. The particles of the hard component are, however, capable of traversing lead plates without producing secondaries. These particles cannot be assumed to be electrons.

According to the theory of collision radiation, the cross-section for radiative collisions for particles of constant energy is inversely proportional to the square of the rest mass of the colliding particle. The small radiation loss suffered by the penetrating cosmic ray particles shows, therefore, that these particles have masses exceeding that of electrons.

(iii) The penetrating cosmic ray particles are now known to be mesons with a mass of about 200 m_e. Before the experimental discovery of the meson, two alternative hypotheses as to the nature of the hard component were considered:

(1) It was suggested that the penetrating particles are electrons, but that the theory of radiation loss breaks down for energies above 100 MEV. This hypothesis seemed to be supported by the fact that most penetrating particles have energies exceeding 200 MEV/c, while most soft particles have energies below this limit. It has been shown, however, since that in fact the spectra of hard and soft particles overlap; in particular, particles losing energies like electrons with energies much exceeding 200 MEV were observed. Thus penetrating and soft particles in the same energy region have been observed, showing that the different behaviour of these particles cannot be accounted for in terms of their energy.

Furthermore, it was pointed out by Williams (1937) that a breakdown of the radiation formulae at high energies is quite unlikely from general consideration. Considering, namely, a radiative collision in the rest system of the radiating electron, it is found that the collision in this system is essentially one within the well-established range of validity of the theory. The high energies which appear in the rest system of the observer are merely introduced by the Lorentz-transformation from the rest system of the electron to the rest system of the observer.

(2) Alternatively, it was suggested that the penetrating particles might be protons. This assumption was rendered difficult, as the negatively charged penetrating particles would have to be assumed to be negative protons, while no experimental evidence for the occurrence of slow negative protons is available. The proton hypothesis was finally ruled out by the fact that many fast penetrating particles with momenta between 1000 and 100 MEV/c are found. Protons in this region could not be fast, and according to (1), such protons ought to ionise heavily. Thus the penetrating particles between 100 and 1000 MEV/c have to be assumed to be lighter than protons on account of their ionisation and heavier than electrons on account of their small radiation loss.

(3) A particle, the mass of which could be shown to be intermediate between that of the electron and the proton, was found by Neddermeyer and Anderson (1938). The particle showed heavy ionisation, and was therefore slow, while its momentum was somewhat below 100 MEV/c. This particle was the first direct evidence for the existence of mesons.

Tracks of slow mesons were since found by a number of other observers. Such tracks are very rare, as the remaining range of a slow meson is very short, and, therefore, the probability of observing a meson very near the end of its range is necessarily small. Observations so far reported, permitting accurate determination of the mass of the meson, suggest a mass of

$$\mu = (180 \pm 20)\, m_e \qquad \ldots\ (5)$$

(m_e = electron mass.)

C. *The Meson.*

(a) *Yukawa's theory.*

Nuclear Forces.

The meson was predicted from purely theoretical consideration by Yukawa (1935) in an attempt to give a theory of inter-nuclear forces and of β-activity. The nucleons (i.e. protons and neutrons) are supposed to carry a "meson charge" acting as the source of a field which may be called the meson field. The relation between meson charge and meson field is somewhat analogous to the relation between charges and field in the electro-magnetic case. The Laplace-Poisson equation representing Coulomb's law is replaced in the meson case by

$$\nabla^2 \phi = \lambda^2 \phi$$

where ϕ is the meson potential, and λ is a parameter of the dimensions of an inversed length. The meson potential due to a point charge is thus obtained as:

$$\varphi = \frac{e^{-\lambda r}}{r}.$$

Thus the meson field gives rise to short range forces with a range of the order of $1/\lambda$. As the range of the nuclear forces is known to be of the order of $e^2/m_e c^2$, one expects as an order of magnitude relation

$$1/\lambda \approx e^2/m_e c^2 \qquad \ldots. \quad (6)$$

The meson field thus described is essentially classical; it does not contain $\hbar$. By quantising the field it is found that the quanta of the meson field have a finite rest mass, and that the parameter $1/\lambda$ plays the rôle of the de Broglie wave-length of the quantum; thus

$$1/\lambda = \hbar/\mu c \quad (\mu = \text{mass of quantum}) \qquad \ldots. \quad (7)$$

From (6) and (7) one finds for the order of magnitude of the mass μ of the quantum

$$\mu \sim 137\, m_e \qquad \ldots. \quad (8)$$

The quantum of the meson field is identified with the meson.

The nuclear forces arising from the meson interaction were assumed to be essentially exchange forces, protons and neutrons interchanging their state of charge by means of emission and reabsorption of virtual mesons. The mesons themselves must hence be assumed to carry electric charges.

The existence of neutral mesons or neutrettos was postulated later in order to account for the forces between like nucleons (Arley and Heitler (1938), Kemmer (1938b)).

Instability of the Meson.

(i) In order to account for the β-activity of some nuclei, Yukawa postulated further that the meson is unstable. It was assumed that mesons decay into an electron and a neutrino after an average life of about $0{\cdot}2 \times 10^{-6}$ sec.

Later calculations have shown that the half-life of the meson ought to be of the order of 10^{-8} sec. in order to account for the β-life times (Nordheim (1939)).

The meson observed in cosmic rays is found experimentally to be unstable. The life of the meson observed with stationary particles is found to be

$$\tau = 2{\cdot}1 \pm 0{\cdot}15 \times 10^{-6} \text{ sec.} \qquad \ldots . \quad (9)$$

(Rossi and Nereson),

thus the observed lifetime is too long to account for the β-decay. In spite of this discrepancy, the striking analogy between the predicted properties of the Yukawa particle and the observed properties of the meson makes it very likely that the cosmic ray particle is in fact identical with Yukawa's particle.

(ii) It was shown by Kemmer (1938a) that there are four different possibilities for the formulation of the meson field. Firstly, the "meson field strengths" can be derived as the (four-dimensional) gradient of a scalar potential. Secondly, in close analogy to Maxwell's equations, the field strength can be obtained from potentials represented by a four vector. In the third and fourth case the potentials are assumed to be a pseudo-vector (i.e. tensor of the third rank), and a pseudo-scalar (i.e. tensor of the fourth rank).

In an attempt to eliminate divergency difficulties arising in the meson theory and also in order to account for the discrepancy between observed and expected life of the meson, Möller and Rosenfeld (1940) put forward the hypothesis that the actual meson field consists of the superposition of two fields, a vector field and a pseudo-scalar field. It is assumed that the pseudo-scalar mesons (i.e. the quanta of the pseudo-scalar field) are the ordinary mesons observed in cosmic rays, while the vector mesons are supposed to have a lifetime of the order of 10^{-8} sec. It is further assumed that the pseudo-scalar meson has a spin 0 while the vector meson has a spin 1.

No experimental evidence for short-lived mesons has been obtained so far, though no evidence against the occurrence of such mesons can be brought forward.

(b) *The experimental meson.*

Evidence that the penetrating component of cosmic rays consists of particles with a mass intermediate between electron and proton has been discussed above (page 9). We now describe the main experiments which show that the meson is unstable.

(i) Direct evidence for the instability of the meson was obtained by Williams and Roberts (1940). These authors obtained a cloud chamber photograph showing a decay electron emitted from the end of the track of a slow meson. A small number of photographs of this kind have been obtained since by other authors.

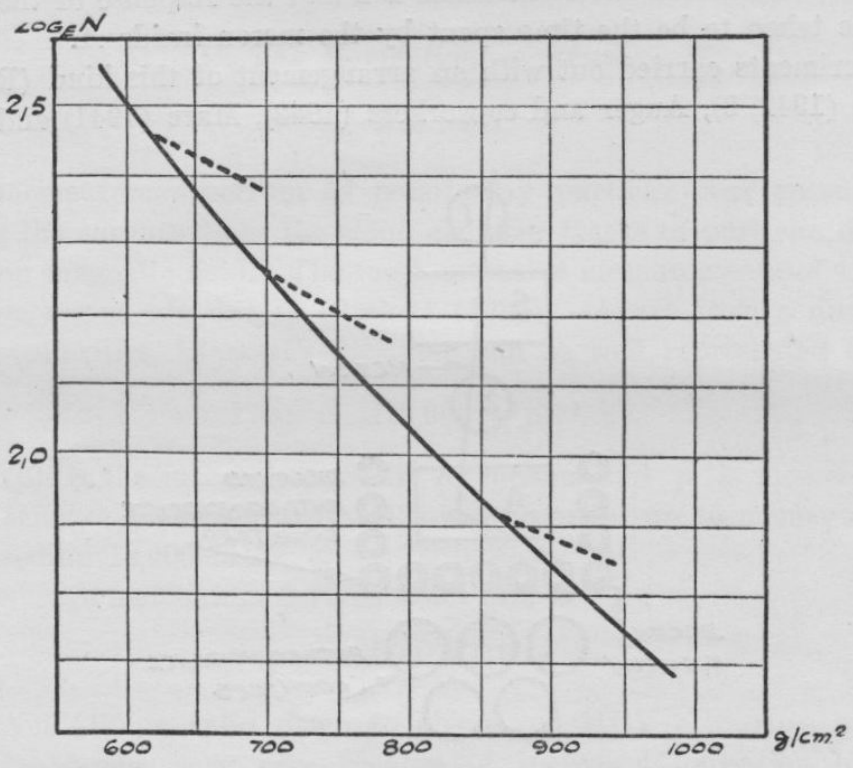

FIG. 6.—ABSORPTION ANOMALY (ROSSI, HILBERRY AND HOAG).

(ii) Indirect evidence of the instability of the meson was obtatined in experiments based on an absorption anomaly.

A beam of mesons traversing a dense absorber is gradually absorbed, due to loss of energy of the particles by ionisation. A beam of mesons passing through an absorber of low density is absorbed partly by ionisation loss, but the loss of particles by decay is also noticeable, provided the time of passage through the absorber is sufficiently long. Thus the rate of absorption of mesons in a gas is larger than the corresponding rate of absorption in a dense absorber of equivalent mass. In the latter case, loss by decay can be neglected.

Experiments of Rossi and co-workers, Neher and Stever, and others show clearly the occurrence of such an anomaly. The results of Rossi and co-workers are reproduced in fig. 6.

From the analysis of the absorption anomaly, the half-life of the meson can be derived. A value of the order 10^{-6} sec. (see Equation (9)) is thus obtained.

(iii) The half-life of the meson was also measured directly with an experimental arrangement shown schematically in fig. 7. An absorber A is placed under a coincidence arrangement 1–2. A meson entering the absorber A may be stopped in A and decay shortly afterwards. The decay electron is likely to discharge one of the counters a surrounding A. Such a process is observed as a coincidence 1–2, followed shortly after by the discharge of one of the counters a surrounding the block A, the time interval between the coincidence 1–2 and the response of the counter a can be taken to be the time spent by the meson inside A.

Experiments carried out with an arrangement of this kind (Rossi and Nereson (1942, 3), Auger and co-workers (1942), Maze (1941) and others),

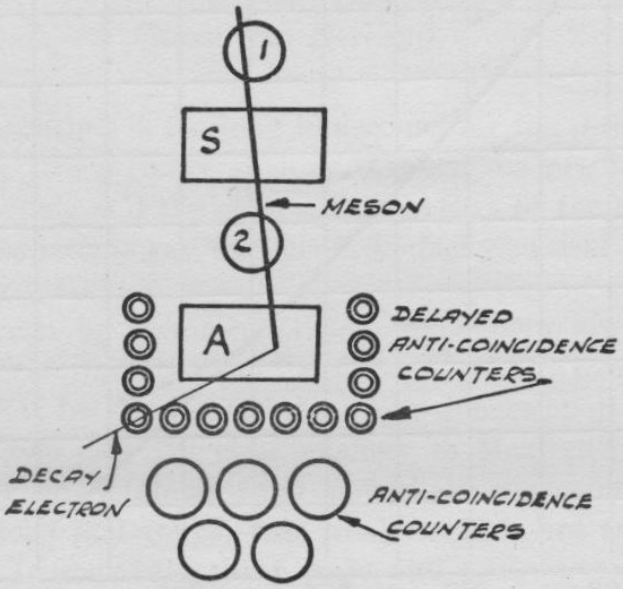

FIG. 7.—ARRANGEMENT FOR THE OBSERVATION OF MESON DECAY.

showed that the fraction of mesons decaying after an interval exceeding t is proportional to

$$e^{-t/\tau} \qquad \ldots\ (10)$$

with $\tau = 2{\cdot}1 \times 10^{-6}$ sec., as given in Equation (9). From (10) it is seen that the delay times are distributed like those of radioactive decay.

It is interesting to compare the experiments described in sections (ii) and (iii). While the former experiments give the proper lifetime of fast mesons, the latter lead to the life of mesons at rest. Because of the relatavistic time contraction, the apparent life τ' of a meson of momentum p is given by

$$\tau' = (p/\mu v)\tau \qquad \ldots\ (11)$$

For an average cosmic ray meson, the time contraction gives rise to a factor of the order of 30. This time contraction is clearly shown when comparing the results of the lifetime as obtained from the absorption anomaly and as obtained from the measurement of the life of a meson at rest.

We note that the observation of the life of the meson in motion and at rest is the first direct experimental evidence for the relatavistic time contraction in a region where this contraction is not causing a small correction but is giving rise to a large effect.

D. *The Momentum spectrum.*

(a) *Sea-level.*

The momentum spectrum of cosmic ray particles was measured by observing the curvatures of the cloud chamber tracks of particles deflected in a strong magnetic field. The most extensive measurements of the high momentum region are due to Blackett (1937). Apart from a number of small irregularities, Blackett's spectrum can be well represented by

$$T(p) = A(2{,}000 + p)^{-1\cdot 5} \qquad \ldots\ (12)$$

where $T(p)$ is the integral spectrum of mesons and p is momentum in units of MEV/c. The spectrum (12) was observed up to momenta somewhat exceeding 10,000 MEV/c.

The average momentum derived from (12) is

$$p = 3000 \text{ MEV/c.}$$

Equation (12) is valid down to about 200 MEV/c, mesons of lower momentum become very rare because of increased ionisation loss and because of decay. The particles below 100 MEV/c are mainly electrons. Their spectrum was investigated by Williams and others.

(b) *Primary spectrum.*

(i) Information about the primary cosmic ray spectrum can be obtained from the effect of the magnetic field of the earth upon cosmic rays. According to the theory of the motion of charged particles in the field of a magnetic dipole (e.g. Störmer (1930), Vallarta (1938)), only particles exceeding a given momentum can approach the earth at a given geomagnetic latitude[2] and in a given direction. Considering particles

[2] Geomagnetic coordinates are those measured with respect to the equivalent dipole of the earth's field.

incident in the vertical direction, it is found in first approximation that only particles with momentum exceeding

$$p(\lambda) = 15{,}000 \cos^4 \lambda \text{ MEV/c} \quad \ldots\ldots (13)$$

can approach the geomagnetic latitude λ in a vertical direction. According to (13), at the equator the spectrum of the vertically incident particles is cut out below 15,000 MEV/c. Similarly, the vertical incident spectrum at the geomagnetic latitude of 50° is cut out below 2500 MEV/c. The spectrum above 15,000 MEV/c can thus be regarded as a background, insensitive to latitude, while due to the gradual cut-off of the primaries between 15,000 and 2500 MEV/c, the vertical intensity will decrease on going from the latitude of 50° towards the equator.

The observed cosmic ray intensity increases by about 10% (compare e.g. Clay (1930), Compton (1933)) between equator and the latitude of 50°. For higher latitudes, the intensity remains constant. It must be concluded from the sea-level latitude effect that only 10 % of the sea-level intensity at latitude 50° is due to primaries with momentum below 15,000 MEV/c, the remaining 90% is latitude insensitive, and is therefore due to primaries of at least 15,000 MEV/c.

(ii) Comparing the above estimates for the momentum of the primaries with the observed momentum spectrum of the mesons near sea-level, the following interesting conclusion can be drawn (compare Nordheim (1938) and also Bowen, Millikan and Neher (1937)).

The loss of momentum of a meson passing through the atmosphere must be of the order of 2,000 MEV/c. Hence the mesons reaching sea-level must have started with an average momentum not more than

(average momentum at sea-level) + (ionisation loss in the atmosphere) =

$$3{,}000 + 2{,}000 = 5{,}000 \text{ MEV/c}.$$

The average momentum of the primaries, giving rise to the mesons at sea-level, must be well above 15,000 MEV, as was shown further above. It is, therefore, concluded that the primaries of the mesons give rise to several mesons each, dividing their energy and momentum among the secondaries.

The above argument was used to prove the secondary nature of the hard component at a time before the experimental discovery of the meson. As the meson is known to be unstable, the secondary origin of the meson component has become self-evident. The argument itself is, however, still of considerable interest, as it throws light on the mode of production of the mesons by their primaries.

(iii) The momentum spectrum of all primaries together can be derived from the latitude effect in the following way. It may be assumed that

the total energy coming into the atmosphere is eventually converted into ionisation.[3] The average energy spent in producing an ion pair in air is about 32 e-volts and, therefore, the total inflow of energy at the top of the atmosphere is given by

$$W = 32ev \int_0^\infty J(\theta)\, d\theta \qquad \ldots\ (14)$$

where $J(\theta)$ is the rate of ionisation at a depth θ below the top of the atmosphere. Evaluating the integral (14) from the observed height ionisation curves, the latitude effect of the energy flow can be determined. The points shown in fig. 8 were obtained from the data of Millikan and his co-workers.

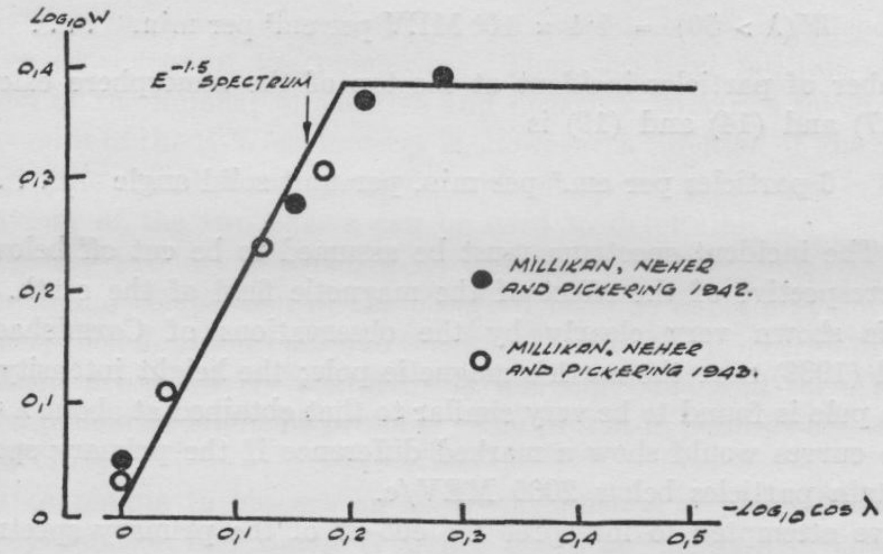

FIG. 8.—HEIGHT INTENSITY DISTRIBUTIONS AFTER BOWEN, MILLLIKAN AND NEHER.

We note that the energy flow is also given by

$$W(\lambda) = -\int_{w_{\min(\lambda)}}^\infty w \frac{dT(w)}{dw}\, dw \qquad \ldots\ (15)$$

where T is the integral spectrum and $w_{\min}$ the limit imposed by the earth's magnetic field. Putting

$$w_{\min} = cp(\lambda) \qquad \ldots\ (16)$$

[3] This assumption is not altogether justified for two reasons.

(1) Some of the energy is converted into low frequency photons and is converted directly into heat.

(2) In the process of meson decay neutrinos are emitted and it is unlikely that the energy of the neutrinos is converted into ionisation.

The effect (1) is unimportant, as was shown by Williams. The energy lost into neutrinos is more important. It is, however, likely that the fraction of energy converted into neutrinos is independent of latitude.

and

$$\begin{aligned} T(w) &= Aw^{-1.5} && w > 2{,}000 \text{ MEV/c} \\ &= 0 && w < 2{,}000 \text{ MEV/c} \end{aligned} \quad \ldots\ldots \quad (17)$$

we find from (13), (15) and (16)

$$\begin{aligned} W(\lambda) &\longrightarrow \frac{1}{\cos^2\lambda} && \lambda < 50^\circ \\ &= \text{const.} && \lambda > 50^\circ \end{aligned} \quad \ldots\ldots \quad (18)$$

We have plotted (18) in fig. 8. It is seen that the agreement between the observed points and the calculation based on the spectrum (17) is satisfactory.

Incidentally, the total flow of energy at high latitudes is found to be (Millikan and co-workers (1943)):—

$$W(\lambda > 50) = 1{\cdot}4 \times 10^5 \text{ MEV per cm}^2 \text{ per min.} \quad \ldots\ldots \quad (19)$$

the number of particles incident at the top of the atmosphere calculated from (17) and (14) and (19) is

$$6 \text{ particles per cm.}^2 \text{ per min. per unit solid angle} \quad \ldots\ldots \quad (20)$$

(iv) The incident spectrum must be assumed to be cut off below 2000 MEV irrespective of the effect of the magnetic field of the earth. This cut-off is shown very clearly by the observations of Carmichael and Dymond (1939) near the earth's magnetic pole; the height intensity curve near the pole is found to be very similar to that obtained at about $\lambda = 50^\circ$. The two curves would show a marked difference if the primary spectrum did contain particles below 2000 MEV/c.

I have attempted to interpret the cut-off of the primary spectrum in terms of the blocking effect of the sun's permanent magnetic field (Jánossy (1937)); this suggestion was taken up by Vallarta (1937) and Epstein (1938). Implications of this theory were later discussed by Vallarta (1939), Jánossy and Lockett (1941).

It appears that no experimental evidence can be brought forward against the assumption that the sun's magnetic field is responsible for the latitude cut off.[4] Experimental evidence as to the existence of a solar dipole field has been obtained recently.

---

[4] The latitude cut off cannot be accounted for, as was suggested by Hamilton, Heitler and Peng (1943) to be due to the lack of meson production below 3000 MEV: the *total flow* of energy into the atmosphere remains namely constant for high latitudes; the total flow of energy is, however, independent of what transformations of the radiation are taking place inside the atmosphere. Thus, if the primary spectrum was not cut off outside the atmosphere, then either the primaries or their secondaries (i.e. the mesons) would show a latitude effect beyond the latitude of 50°, contrary to the observed facts. It must be concluded, therefore, that the low energy cut off is imposed on the primaries before they enter the atmosphere.

(c) *Positive and negative primaries.*

(i) The forbidden directions for positively charged particles are predominantly to the east, while the forbidden direction for primaries with negative charge are predominantly to the west. Therefore, positive primaries are expected to give rise to higher intensity in directions inclined to the west than in the directions inclined correspondingly to the east. Negative primaries are expected to give rise to an opposite asymmetry.

(ii) Observations by Johnson (1938) and others have revealed an excess of intensity from the west, both at sea-level and for observations carried out at altitudes up to 4000 *m* above sea-level. From these observations it must be concluded that the primaries must contain more positively charged particles than negatively charged ones.

The ratio between positively and negatively charged primaries can in fact be estimated fairly accurately by comparing the latitude effect with the E–W–asymmetry. The shape of the latitude effect is independent of the sign of charge of the primaries. Thus the total latitude effect is a function of the number of positive and negative primaries taken together. The amount of the E-W-asymmetry is, however, a function of the *difference* between the number of positive and negative primaries. Thus the comparison of the two effects can be used to determine the positive and the negative primary intensities separately.

The actual comparison of the observed latitude effect and the observed asymmetry led Johnson (1939) to conclude that all the primaries of the hard component are positively charged. It was suggested that these positively charged primaries might be protons. The proton hypothesis has won much ground lately.

(iii) Attempts to observe an E–W–asymmetry at high altitudes were made by Johnson and Barry (1939). The experiments had, however, an entirely negative result; no asymmetry outside the limits of experimental accuracy could be observed. At great heights the soft component is predominant; therefore Johnson's results indicate that the soft component shows no asymmetry. The simplest interpretation of the lack of asymmetry of the soft component is obtained by assuming that the soft component is due to positive and negative primary electrons. (The primaries of the soft component could not be photons, as the soft component shows a marked latitude effect.)

Incidentally, Johnson's results make it very likely that the soft and hard components do not arise from common primaries.

E. *The soft component.*

Apart from mesons, the cosmic ray beam contains electrons and photons which form the soft component. This latter component is strongly absorbed, especially in heavy elements, due to the emission of quanta by

electrons, and the absorption of quanta with subsequent production of electron pairs.

An energetic electron falling on an absorber will thus give rise to a number of quanta; the quanta in their turn will give rise to electron pairs; thus an electron passing through an absorber will give rise to many secondaries. In this way energetic electrons (or photons) are giving rise to showers.

(a) *Experimental investigation of showers.*

Indications that cosmic ray particles have a tendency of forming groups were found already by Skobelzyn (1929); some of his first photographs contained the tracks of two or three simultaneous cosmic ray particles.

Beautiful photographs of very complex showers were later obtained by Blackett and Occhialini (1933), Anderson (1933) with the counter controlled cloud chamber. Many cloud chamber investigations into the properties of the cosmic ray showers have been carried out since.

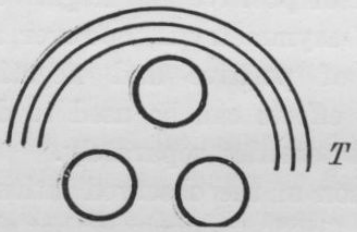

FIG. 9a.—TRIPLE COINCIDENCE ARRANGEMENT AFTER ROSSI.

Rossi transition.

Independently of the cloud chamber work, showers were investigated in detail by Rossi (1933). Rossi used various counter arrangements for his investigation; a typical arrangement is shown in fig. 9a.

The arrangement (fig. 9a) consists of three counters placed on the corners of a triangle. At least two particles are required to discharge all

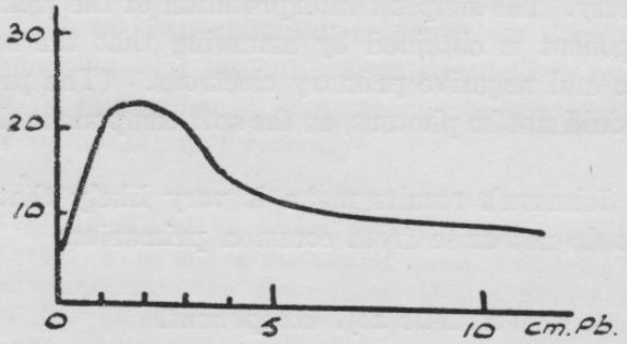

FIG. 9b.—TRANSITION EFFECT (SCHEMATICAL).

the three counters simultaneously. Threefold coincidences of this arrangement are therefore attributed to showers.

An absorber T is placed close above the counters. It is found that the rate of threefold coincidences varies with varying thickness of T. The rate of coincidences as function of the thickness of the absorber T is also shown in fig. 9b. The rate increases strongly with increasing absorber up to a thickness of about 1·5 cm. of lead. For larger thicknesses, the rate decreases again. For large thickness, i.e. larger than 7 to 10 cm. of lead, the rate remains nearly constant.

The effect shown in fig. 9b is usually termed the Rossi transition effect.

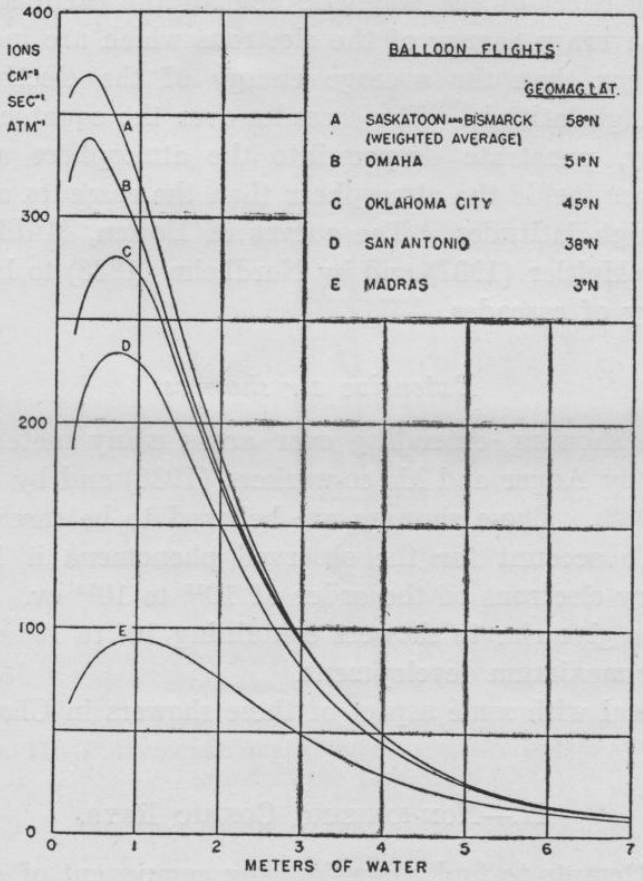

FIG. 10.—THE LATITUDE EFFECT OF THE ENERGY FLOW.
Observed and calculated for $E^{-1,5}$ spectrum.
[Reproduced from *Phys. Rev.*, **61**, 405 (1942).]

It is due to the development and subsequent absorption of showers falling on the absorber T. The extended tail of the Rossi transition curve is due to showers which are secondary to the hard component.

Cascade Theory.

The shower phenomena were interpreted in terms of electrons and photons by Bhabha and Heitler (1937) and by Carlson and Oppenheimer (1937). These authors showed that most of the shower phenomena can

be accounted for in terms of cascades started by electrons or photons. In particular, the height intensity distribution of the cosmic ray beam can be largely accounted for as the atmospheric transition curve of a primary electron component. In fig. 10 we have reproduced the height intensity curves at various latitudes, as observed by Bowen, Millikan and Neher (1957, 8). We note that the maximum of the intensity lies deeper down in the atmosphere when observing over the equator than it lies when observing at a high latitude. This effect is simply accounted for in terms of the blocking effect of the magnetic field of the earth and the cascade theory:—The average energy of the electrons which are incident over the equator is larger than the average energy of the electrons which are incident at a high latitude. The cascades over the equator, having larger average energy, penetrate deeper into the atmosphere and produce a maximum deeper inside the atmosphere than the cascades of lower energy occurring at high latitudes. The curves of Bowen, Millikan and Neher were found by Heitler (1937) and by Nordheim (1938) to be in agreement with the theory of cascades.

Extensive air showers.

Very large showers, extending over areas many meters in diameter, were observed by Auger and his co-workers (1938) and by Kolhörster and co-workers (1938). These showers are believed to be cascades developing in the air. To account for the observed phenomena it is necessary to assume primary electrons of the order of 10^{15} to 10^{16} ev. Such electrons are expected to give rise to showers containing 10^6 to 10^7 electrons in the region of their maximum development.

We shall deal with some aspect of these showers in Chapter VI.

II.—Non-ionising Cosmic Rays.

The first attempts to find a non-ionising component of cosmic rays are due to Rossi (1931). In these experiments a counter arrangement shown schematically in fig. 11 was used. Threefold coincidences 1–2–3 were observed with an absorber S alternatively placed into the positions I (above the top counter) and II closely below the top counter.

It was argued that non-ionising rays giving rise to ionising secondaries in S could be recorded with S in the upper position, but they could not be recorded with S in the lower position. Non-ionising rays giving rise to ionising secondaries would, therefore, contribute to a difference of the counting rates with S in the positions I and II.

Rossi observed a small increase of the counting rate when moving S from II to position I. Realising, however, that a small difference of this type might be caused by effects other than non-ionising rays, Rossi

did not conclude that his observations were to be interpreted in terms of non-ionising rays.

Many experiments of this type were carried out by others. The latter arrangements were designed much less critically than that of Rossi, and, therefore, the very contradictory results obtained by various authors did not yield any reliable information as to the existence of non-ionising cosmic ray particles. Significant results showing the existence of non-ionising components were obtained later by replacing the coincidence arrangements by anticoincidence arrangements. We describe the latter method, suggested by Rossi, in the following section.

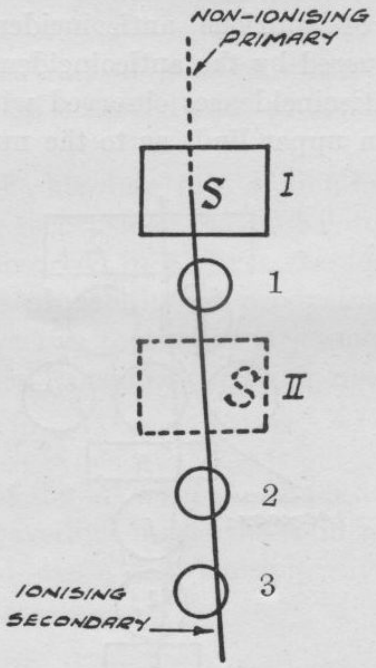

FIG. 11.—COINCIDENCE ARRANGEMENT FOR THE OBSERVATION OF NON-IONISING RADIATION.

A. *The anticoincidence method.*

The main shortcoming of the coincidence experiments concerning effects of non-ionising rays is the fact that the absorber S has to be moved in the course of the experiment. By moving any part of the arrangement the background due to scattered particles, showers, etc., is necessarily affected by an unknown amount, and masks any effect due to non-ionising rays. Rossi suggested, therefore, the use of anticoincidence counters for the observation of non-ionising rays. The method is explained below:—

(i) An anticoincidence arrangement is shown schematically in fig. 12. Anticoincidences 1–2–3–A are recorded. An anticoincidence 1–2–3–A is a coincidence of the counters 1–2–3 which is *not accompanied* by the discharge of any of the anticoincidence counters A.

Anticoincidences may be caused by a number of effects. One of the possible causes of an anticoincidence is a non-ionising ray falling on the absorber S below the anticoincidence counters, and giving rise to a secondary in S, which in its turn discharges the counters 1–2–3. This type of anticoincidence is the only one which is of interest in the following, and we shall call it a *genuine* anticoincidence. Anticoincidences due to other causes will be termed *spurious* anticoincidences. Spurious anticoincidences are caused, for instance, by showers coming from the side discharging the counters 1, 2, 3, but missing the counters A. Another source of spurious anticoincidences is a particle hitting S from the side and being scattered into the solid angle subtended by the coincidence counters. The rate of spurious anticoincidences can be reduced by extending the areas covered by the anticoincidence counters.

(ii) The rate of anticoincidences observed with an arrangement of the type of fig. 12 gives an upper limit as to the number of non-ionisng rays

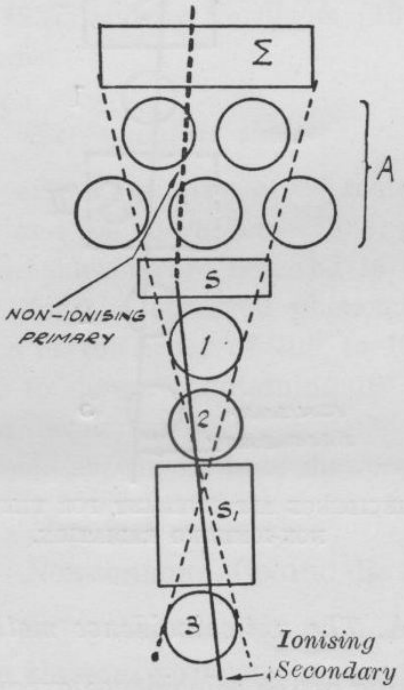

FIG. 12.—ANTICOINCIDENCE ARRANGEMENT FOR THE OBSERVATION OF NON-IONISING RADIATION.

producing secondaries in S. The following method has proved useful in establishing what fraction of the observed anticoincidences can be taken to be genuine. On placing the absorber Σ close above the anticoincidence counters, the rate of genuine anticoincidences is reduced, since non-ionising rays will give rise to ionising secondaries in Σ, and may be absorbed in doing so. (Even if a non-ionising particle is not absorbed when giving rise to the ionising secondary in Σ, still the presence of the ionising secondary prevents the non-ionising particles from being counted as an anticoincidence.)

The rate of spurious anticoincidences is unlikely to be affected by the presence of the absorber Σ. Therefore, a substantial reduction of the anticoincidence rate due to an absorber Σ placed close above the anticoincidence counters can be taken as evidence for the occurrence of genuine anticoincidences.

(iii) Recording the rate of anticoincidences as a function of the thickness x of Σ, the mean free path of the non-ionising rays can be determined. Write αdx for the probability of an ionising secondary being produced along dx. The probability of a non-ionising ray traversing the whole of the absorber Σ without encounter is then

$$P(x) = e^{-\alpha x}.$$

$P(x)$ is proportional to the rate of genuine anticoincidences, and thus α can be determined from the observed rate of change of anticoincidences with x.

In order to estimate the absolute rate of non-ionising rays falling on the arrangement, one has to consider the probability that a non-ionising ray, which has not been absorbed in Σ, gives rise to an ionising secondary in S. Assuming that the probability of producing a suitable secondary in S is the same as to give rise to a secondary emerging from Σ, we find for the probability of a non-ionising ray giving rise to an anticoincidence

$$P = e^{-\alpha x}(1 - e^{-\alpha y}) \qquad \ldots\ (21)$$

where y is the thickness of the absorber S. Equation (21) gives the ratio of all non-ionising rays travelling inside the solid angle subtended by the coincidence counters, and those non-ionising rays which actually are recorded by anticoincidences.

B. *The Photon Component.*

Experiments of the type described above with the object of studying the photon component of cosmic rays were carried out by Jánossy and Rossi (1940) and by Trumpy (1943).

In the experiments of Jánossy and Rossi, the absorber S (fig. 12) was chosen about 2 cm. thick. A considerable rate of anticoincidences was observed, without any absorber Σ above the anticoincidence counters. A few cms. of lead in position Σ reduced the rate of anticoincidences to about one-half. It was, therefore, concluded that about 50% of the observed anticoincidences were genuine.

From the dependence of the anticoincidence rate upon the thickness of Σ in the actual experiment, it could be shown that the non-ionising rays are absorbed like photons; both the absolute cross-section and the dependence of the cross-section on the atomic number Z of the absorber were found to agree with the theory of Bethe and Heitler.

These experiments thus proved the existence of a photon component of cosmic rays and at the same time gave a direct experimental verification of the Bethe-Heitler theory.

Further, arranging the coincidence counters in a triangle (fig. 13), the arrangement could be made selective for showers produced in S by incident photons. By varying the thickness of S, the transition effect of photon-produced showers could be studied. (Compare Nereson (1942), Trumpy (1943), Jánossy and Rossi (1940)).

Finally, it was found that genuine anticoincidences disappeared when an absorber S_1 of about 8 cm. lead was placed between the counters of the coincidence arrangement (fig. 12). This experiment proves that

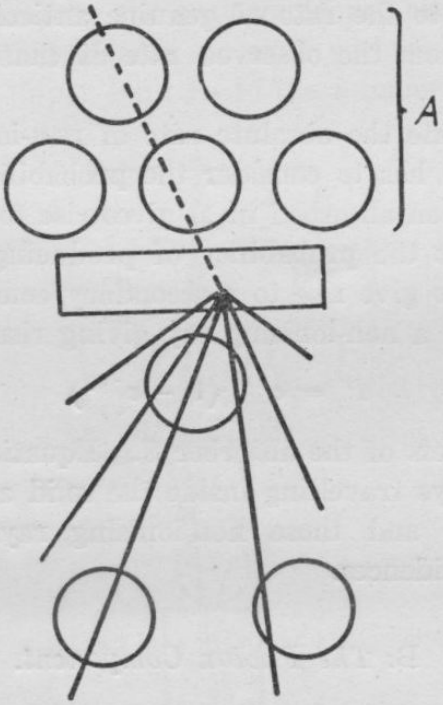

FIG. 13.—ANTICOINCIDENCE ARRANGEMENT FOR THE OBSERVATION OF PHOTON PRODUCED SHOWERS.

photons do not give rise to an appreciable number of penetrating particles. The soft cascade showers produced in S are, of course, all absorbed in the absorber S_1.

C. *Penetrating Non-ionising Rays.*

(1) Rossi and Regener (1940) carried out experiments with an arrangement of the type described in fig. 12 at Mt. Evans, 4300 m. above sea-level. The rate of anticoincidences showed the usual reduction due to photons while the absorber Σ was increased from 0 to 2·5 cm. of lead. The anticoincidence rate showed, however, a further significant reduction while Σ was increased from 2·5 to 7·5 cm. of lead. This

decrease could not be accounted for in terms of photons, and it was concluded that it was caused by the absorption of non-ionising rays more penetrating than photons.

(ii) More extensive experiments leading to the same conclusion were carried out near sea-level by Jánossy and Rochester (1942). The penetrating non-ionising component near sea-level was found to be very weak, and, therefore, extensive precautions had to be taken in order to reduce the background, due to spurious anticoincidences.

The arrangement used by Jánossy and Rochester (1943a) is shown schematically in fig. 14. The coincidence counters 1, 2, 3 are surrounded from five sides by a box of anticoincidence counters. The box consisted of 76 counters in parallel. Every ray giving rise to a coincidence 1–2–3 must necessarily traverse the surrounding anticoincidence counters, and,

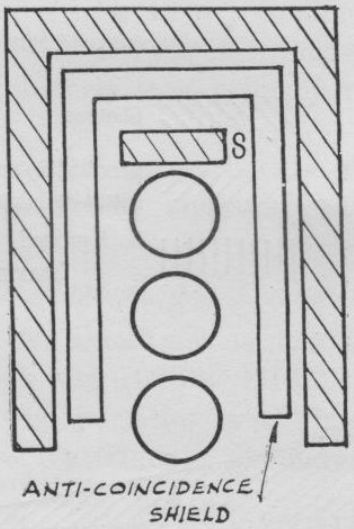

FIG. 14.—SCHEME OF ARRANGEMENT OF JÁNOSSY AND ROCHESTER FOR THE INVESTIGATION OF PENETRATING NON-IONISING RADIATION.

therefore, no ionising rays coming from outside are capable of giving rise to anticoincidences. The "leakage" of ionising particles arising from the inefficiency of the counters could be reduced to less than 0·3 of a per cent—i.e. not more than three particles out of 10,000 could enter the anticoincidence box undetected.

An absorber *S* was placed close above the coincidence counters. Anticoincidences were thus given rise to by non-ionising rays from outside, giving rise to ionising secondaries in *S*.

Most of the anticoincidences recorded with an unshielded arrangement are due to photons. In order to cut out the contribution of photons, the anticoincidence counters were further surrounded with a lead absorber 5 cm. thick. Photons traversing 5 cm. of lead are unlikely to emerge unaccompanied by electrons. Therefore the lead absorber cuts out effectively all genuine anticoincidences due to photons.

About half of the anticoincidences observed under the 5 cm. lead shield could be shown to be genuine by placing further lead absorbers Σ on top of the 5 cm. lead box. The rate of anticoincidences as function of the thickness of Σ is shown in fig. 15. It is seen that the anticoincidence rate drops significantly when Σ is increased from 5 to 35 cm. of lead. Whether or not all the anticoincidences observed under 35 cm. of lead are spurious could not be decided.

The following properties of the penetrating non-ionising rays could be inferred from the above experiments :—

(1) The mean free path of these rays must exceed 5 cm. of lead, and

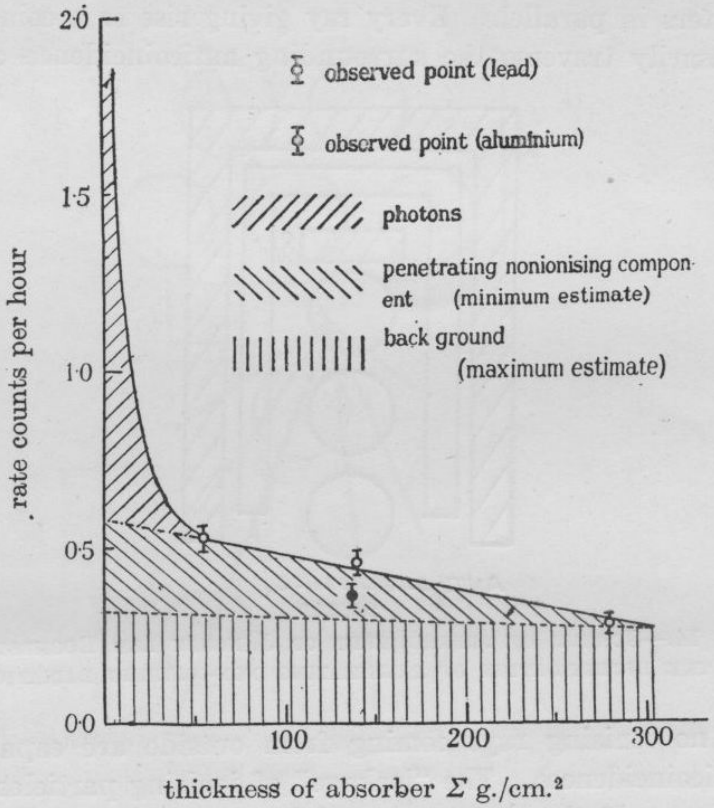

FIG. 15.—EXPERIMENTAL RESULTS OBTAINED WITH THE ARRANGEMENT IN FIG. 14.

[Reproduced from *Proc. Roy. Soc.*, **A**, **181**, 404 (1943).]

is probably less than 35 cm. of lead. The absorption curve, fig. 15, makes a mean free path of about 10 cm. of lead not unlikely.

(2) The intensity of the penetrating non-ionising component at sea-level appears to be about 1/700th of the total cosmic ray intensity. (This estimation refers only to directions of incidence near the vertical direction.)

(3) Comparing the results of Rossi and Regener at Mt. Evans and those near sea-level by Jánossy and Rochester, it can be shown that the intensity between the two stations is reduced by a factor between 30

and 60. From this absorption, it is estimated that the mean free path in air of the non-ionising particles is of the order of 100 g. per cm.^{2}.

From (1) and (3) it is inferred that the absorption of the penetrating non-ionising rays is roughly proportional to mass. The reduction of the rate of anticoincidences caused by 15 cm. of Al is also compatible with the assumption of mass absorption.

III.—Penetrating Showers.

Most of the showers observed at sea-level are cascade showers consisting of electrons and photons. Such showers are soft—i.e. most of the cascade showers are absorbed in a few cms. of lead; very few cascades have ranges exceeding, say, 10 cm. of lead.

Besides the ordinary cascades, so-called knock-on showers are observed. Knock-on showers are due to an electron secondary produced by a meson. Similarly, a meson can give rise to a secondary shower by emitting a photon. The characteristic of the knock-on showers is that they contain one penetrating particle, namely, the primary meson giving rise to the shower.

In the following we describe experiments showing the existence of penetrating showers—that is, of showers containing more than one penetrating particle.

A. *Photographic Evidence.*

Photographs showing two simultaneous mesons traversing a lead plate were obtained by Braddick and Hensby (1940). Photographs containing three or more penetrating particles were later obtained by several observers. In fig. 16 we reproduce a photograph obtained by Jánossy, McCusker and Rochester (1941).

Penetrating showers do not always consist of a number of penetrating particles coming from one point. Complicated penetrating showers were obtained by Fussel (1938). We reproduce in figs. 17 and 18 two complicated showers. The photograph, fig. 17, is due to Hazen. The shower is seen to traverse eight metal plates in succession. The photograph, fig. 18, was obtained by McCusker.

B. *Counter investigations into the properties of penetrating showers.*

(a) *The experiments of Wataghin and his co-workers.*

(1) Wataghin and his co-workers (1940) observed fourfold coincidences with an arrangement as shown in fig. 19. The four counters, 1, 2, 3, 4, are placed on the corners of a rectangle. The lower counters 3 and 4 are embedded in lead; they are separated by 17 cm. of lead from the upper counters 1 and 2.

Fourfold coincidences can be produced by showers containing at least two penetrating particles. We shall show that the fourfold coincidences cannot be produced by either knock-on showers nor by cascade showers.

(ii) According to the cascade theory, cascade showers penetrating 17 cm. of lead must have a primary energy of at least 10^7 MEV. Electrons of this energy are expected to be infrequent, but their existence cannot be excluded altogether. An electron of 10^7 MEV, giving rise to a cascade in the lead, could, however, discharge only one of the upper counters and one of the lower counters of the arrangement shown in fig. 17. A fourfold coincidence could only be accounted for in terms of at least *two* electrons both exceeding 10^7 MEV and separated by about 1 m. of the order of the distance between the counters 1 and 2. According to the theory of the extensive air showers (see Chapter VI), the root mean square separation of electrons of energy E is of the order of

$$60m\,(E_c/E) \qquad \ldots\ (22)$$

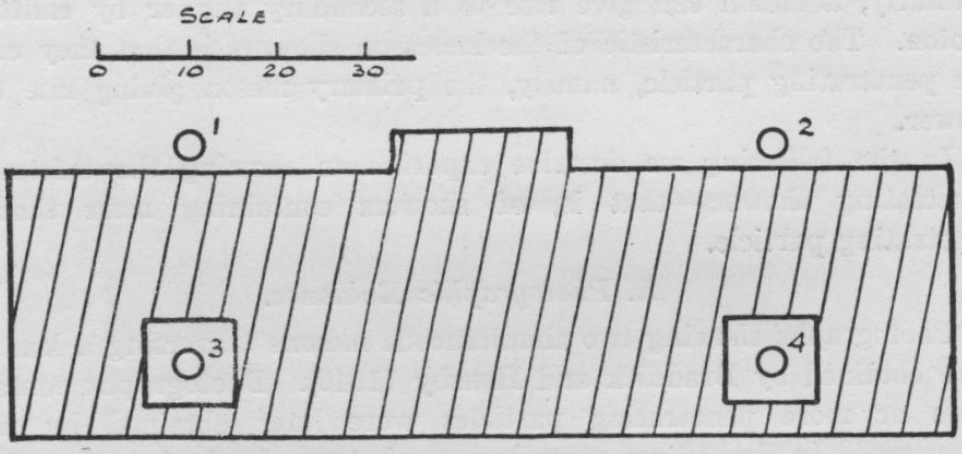

FIG. 19.—THE ARRANGEMENT OF WATAGHIN AND CO-WORKERS.

where $E_c = 100$ MEV, the critical energy in air. Electrons of an air shower exceeding 10^7 MEV are, therefore, separated in air by about

$$60m/10^5 = 0{\cdot}06 \text{ cm.}$$

Hence the electrons of 10^7 MEV are crowded together very closely to the core of the shower. The possibility of an air shower containing 10^7 MEV electrons separated sufficiently to account for a fourfold coincidence 1–2–3–4, can therefore be excluded.

By a similar argument, it can be shown that the fourfold coincidences observed by Wataghin cannot be due to knock-on showers.

Consider a meson discharging the counters 1 and 3 (fig. 19). In order to discharge the counters 2 and 4 as well, the meson must give rise to a knock-on shower with an initial energy of at least 10^7 MEV. Such a shower is initiated at an extremely small angle to the direction of the primary, and the energetic part of the knock-on cascade follows closely the path of the meson. Therefore, the knock-on shower cannot spread

sufficiently far apart from the primary meson so as to complete the fourfold coincidence.

It must be concluded, therefore, that the showers observed by Wataghin are neither knock-on showers nor cascade-showers.[5]

(iii) It was found by Wataghin that a counter placed at a distance of 3 m. from his arrangement was occasionally discharged simultaneously with the main set shown in fig. 19. It can be concluded, therefore, that at least some of the penetrating showers are parts of large showers extending over areas of several meters in diameter.

Further, a counter 5 was placed between the counters 3 and 4. It was found that the rate of fivefold coincidences 1–2–3–4–5 was not much less than the rate of fourfold coincidences 1–2–3–4. From the ratio of the fourfold and fivefold coincidences, it was concluded that the penetrating showers contain a fairly large number of penetrating particles.

(b) *The Experiments of Jánossy and his co-workers.*

Extensive Showers.

(i) The arrangement of Jánossy and his co-workers (1940, 1, 3, 3b, 4) is shown in fig. 20. The counters are arranged in three trays separated

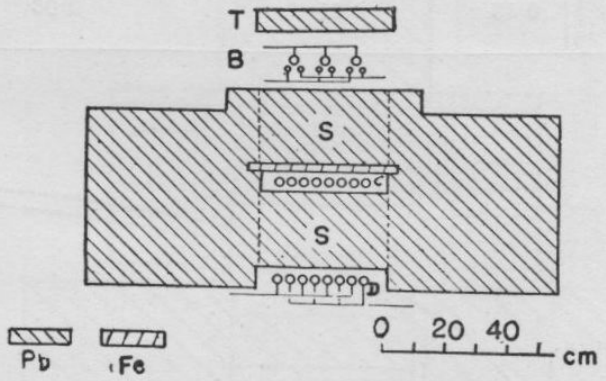

FIG. 20.—THE ARRANGEMENT OF JÁNOSSY AND CO-WORKERS.
[Reproduced from *Phys. Rev.*, **64**, 348 (1943).]

by lead absorbers 15 cm. thick. Sevenfold coincidences containing three counters of the top tray and two counters out of each of the middle and bottom trays were recorded. It was shown in detail (compare Jánossy, 1941) that sevenfold coincidences of this arrangement cannot be due to cascades or to knock-on showers.

(ii) The arrangement, fig. 20, was used both with and without an absorber T placed close above the top counters. Most of the coincidences obtained without the absorber T above the counters are caused by large air showers, as was shown by the following experiment:—

[5] This argument was put forward by Auger and independently by the author.

A counter tray *E* containing several counters in parallel and covering an area of about 2000 cm.^{2} was placed near the main set (*PS*). It was found that (in the absence of an absorber *T*) most of the sevenfold coincidences *PS* are accompanied by the discharge of the tray *E*. The rate of eightfold coincidences *PS, E* proved to be insensitive as to the distance between *PS* and *E* up to 10 m., the largest distance for which observations were actually carried out. From these observations it is concluded that the showers causing the eightfold coincidences contain a large number of particles distributed over an area of more than 10 m. radius.

These large showers do not contain many penetrating particles. It was found that the rate of eightfold coincidences *PS, E* is largely reduced when the tray *E* is covered with a lead absorber 15 cm. thick.

To show the orders of magnitudes, we have collected a few observational data in the table below (Jánossy and Broadbent, unpublished):—

	PS	PS–E unshielded	PS–E (E shielded by 15 cm. Pb) number of counters discharged in the tray E.	
			$\geqslant 1$	$\geqslant 2$
Rate per hour	0·16	0·11	0·03	0·01

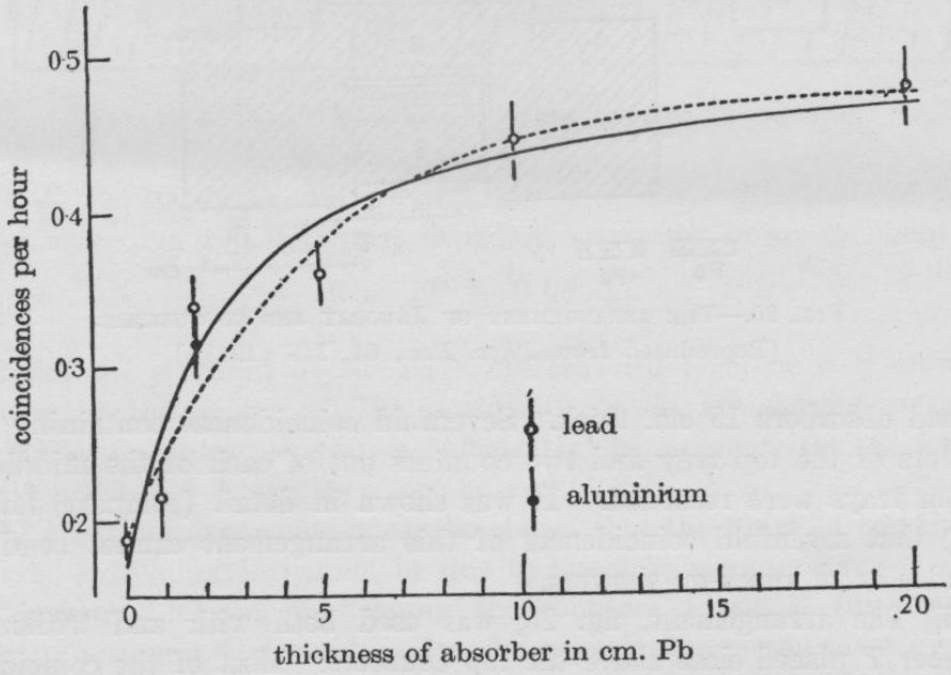

FIG. 21.—THE TRANSITION EFFECT OF PENETRATING SHOWERS (JÁNOSSY AND ROCHESTER).

[Reproduced from *Proc. Roy. Soc.*, **A**, 183, 183 (1944).]

Local Penetrating Showers.

(i) Penetrating showers have a pronounced transition effect; the rate of sevenfold coincidences *PS* increases when absorbers are placed close above the top tray of counters of the arrangement *PS*. The transition effect observed by Jánossy and Rochester (1944) is shown in fig. 21.

The transition effect can be interpreted in terms of production of penetrating showers in the absorber *T* by some primary radiation. The transition effect shows saturation for thicknesses of the order of 5 cm. of lead, thus the mean free path of the primaries must be assumed to be about 5 cm. of lead. Comparison of the transition effects in different materials seems to suggest that the rate of production of penetrating showers is roughly mass proportional. The mean free path of the primaries can be assumed to be of the order of 100 g. per cm.^{2}.

(ii) Whether the primaries giving rise to penetrating showers are ionising or non-ionising was investigated by Jánossy and Rochester (1943b), in the following way :—

A counter arrangement of the type shown in fig. 22 was used. The lower half of the arrangement of fig. 22 is analogous to the arrangement

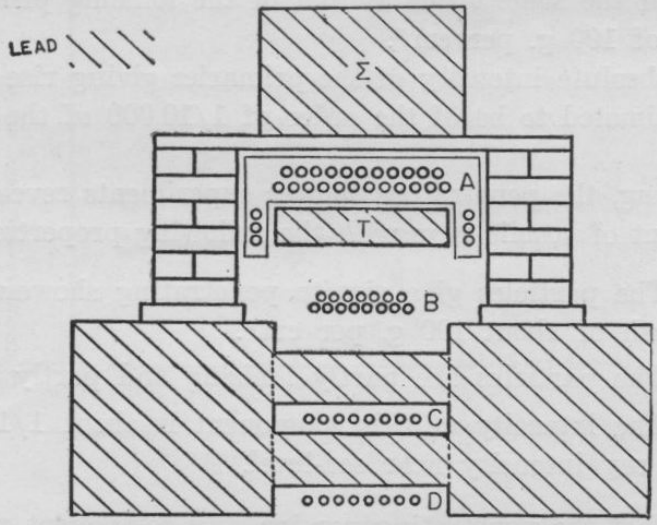

FIG. 22.—ARRANGEMENT FOR THE OBSERVATION OF THE PRODUCTION OF PENETRATING SHOWERS BY NON-IONISING PRIMARIES (JÁNOSSY AND ROCHESTER).

[Reproduced from *Phys. Rev.*, **64**, 348 (1943).]

fig. 20; this arrangement responds mainly to penetrating showers, some of which are produced in the 10 cm. thick lead absorber *T*.

To investigate the nature of the primaries, the absorber *T* was surrounded from five sides by a set of anticoincidence counters *A*. Non-ionising primaries falling on *T* and giving rise to penetrating showers in *T* are expected to give rise to anticoincidences *PS–A*.

A number of anticoincidences *PS–A* were observed with the arrangement, fig. 22. It could be shown that these anticoincidences were genuine, i.e. due to non-ionising primaries and not due to spurious effects of any other kind. It was found, namely, that the rate of anticoincidences *PS–A* decreases greatly when a sufficiently thick absorber Σ is placed above the anticoincidence set *A*. Though the rate of anticoincidences was found to be only little affected by 5 cm. of lead in position Σ above the counters *A*, the rate was considerably reduced by 35 cm. of lead.

From the actual rate of anticoincidences, it was estimated that about one-third of the penetrating showers produced in *T* is due to non-ionising primaries, while the rest is due to ionising particles.

(iii) The mean free path of the non-ionising primaries producing penetrating showers can be estimated from the rate of change of anticoincidences with increasing thickness of Σ.

As the rate of anticoincidences is not much reduced by 5 cm. of lead, it must be concluded that the non-ionising rays are considerably more penetrating than photons. The range of the non-ionising primaries must be less than 35 cm. of lead, as 35 cm. of lead causes a considerable reduction. It is, therefore, plausible to assume that the range of the non-ionising primaries is of the same order as that of the ionising primaries, namely, of the order of 100 g. per cm.^{2}.

(iv) The absolute intensity of the primaries giving rise to penetrating showers is estimated to be of the order of 1/10,000 of the rate of cosmic ray particles.

Summarising, the penetrating shower experiments reveal the existence of a component of cosmic rays with the following properties:—

1. The particles give rise to penetrating showers with a mean free path of about 100 g. per cm.^{2}.

2. The particles are partly ionising and partly neutral.

3. The intensity of this component is about 1/10,000th of the cosmic ray intensity near sea-level.

We add, that the penetrating non-ionising component reported in the previous chapter may consist of particles of the same nature as the non-ionising particles giving rise to penetrating showers.

The intensity of the neutral component reported in Chapter II is much larger than that of the component giving rise to penetrating showers. This difference could be due to the different type of selection in the two experiments. The arrangement, fig. 14, reported in Chapter II is sensitive to fairly low energy neutral particles; this arrangement is capable of recording neutral particles giving rise to an ionising secondary with a range of a few cm. of lead. On the other hand, the arrangement, fig. 20, is only sensitive to neutral particles capable of producing a

penetrating shower containing a number of particles with ranges exceeding 30 cm. of lead. Therefore, the latter arrangement is only sensitive to a much smaller part of the neutral spectrum than the arrangement, fig. 14.

Connexion between local penetrating showers and extensive penetrating showers.

In the following we show that the local penetrating showers and the extensive penetrating showers are two different phenomena; the fact that both can be recorded with similar arrangements is only accidental.

(i) Observations were carried out with the apparatus of fig. 20 recording coincidences *PS* and using the tray *E* (see page 30) as anticoincidence. An anticoincidence *PS–E* is thus a coincidence *PS*, not accompanied by the discharge of any of the (anticoincidence) counters *E*. Such anticoincidences are mainly caused by local showers not accompanied by extensive showers.

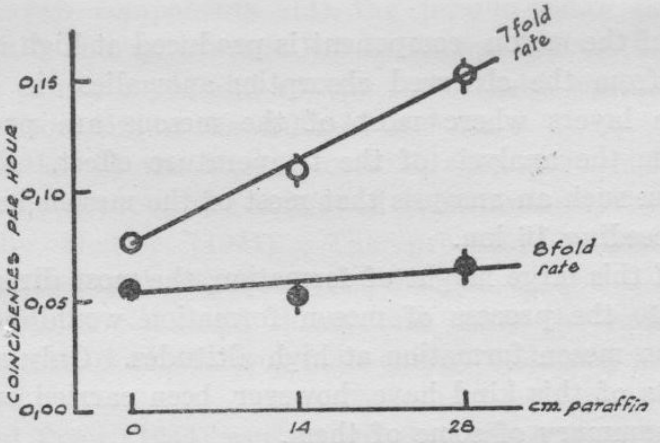

FIG. 23.—TRANSITION EFFECT OF LOCAL PENETRATING SHOWERS (JÁNOSSY AND BROADBENT).

The rate of eightfold coincidences *PS, E* and also the rate of *anticoincidences PS–E* were recorded as function of the thickness of the absorber *T* placed close above the set *PS*. The result of these records is shown in fig. 23. (Unpublished results of Jánossy and Broadbent.) While the rate of anticoincidences, which are due to the local showers, is found to increase appreciably with increasing *T*, the rate of eightfold coincidences, due to extensive air showers, remains unaffected by the variation of *T*. We see, therefore, that the observed coincidences *PS* can be regarded as due to two independent contributions, namely, (1) "background," i.e. eightfold coincidences *PS, E*, the rate of the background is not affected by *T*; and (2) local showers, i.e. anticoincidences *PS–E*.

These anticoincidences are very rare without an absorber T; their rate increases strongly with T.[5a]

(ii) The penetrating extensive showers were investigated by Cocconi (1943) and others. It appears that these showers are large cascades containing a few mesons. It was pointed out by Ferretti[6] that the penetrating particles appearing in extensive air showers may be produced either in the air, or in the absorbers shielding the counters of the penetrating shower arrangements.

(iii) The local penetrating showers are probably groups of mesons produced in the absorber T'. The primaries giving rise to these groups of mesons are probably neutrons and protons, as will be shown in the following chapter.

In fact, photographs taken with a cloud chamber controlled by a penetrating shower arrangement show occasionally groups of mesons coming from a point. An example of such a photograph is reproduced in fig. 16.

C. *Meson production at high altitudes.*

The bulk of the meson component is produced at high altitudes. This can be seen from the observed absorption-anomalies; in particular, the height of the layers where most of the mesons are produced can be estimated from the analysis of the temperature effect. Duperier (1944) concludes from such an analysis that most of the mesons have their origin at heights exceeding 16 km.

Because of this large height of formation, the most direct experimental approach as to the process of meson formation would be to carry out experiments on meson formation at high altitudes. Only a small number of experiments of this kind have, however, been carried out so far. We give a short summary of some of them.

(i) W. H. Regener (1943) used on Mt. Evans an arrangement over 100 self-recording counters arranged in trays separated by absorbers of lead. With this arrangement, Regener finds evidence for the production of mesons singly, and also in groups. The primaries in this process are found by Regener to be mainly non-ionising particles. The cross-section for meson production is found to be of the order of the geometrical cross-section of the nuclei of the producing substance.

Unfortunately, only few details of these experiments have been published.

[5a] More detailed observations have revealed that the extensive showers show a small transition effect in lead but no transition effect in paraffin (Jánossy and Broadbent, 1947).

[6] In conversation with the author.

(ii) Schein, Iona and Tabin (1943) used a complicated counter arrangement to detect the production of mesons and meson showers in paraffin. The arrangement was carried in a balloon up to a height corresponding to 2 cm. Hg. pressure. The experiments reveal that the rate of production of mesons increases considerably with height.

The cross-section for the production of the mesons is found to be of the order 10^{-25} cm.^{2} per atomic nucleus. Unfortunately, the actual results of Schein have not been published in detail.

IV. Interpretation of the Experimental Evidence concerning the Production of Mesons.

A theory of the origin of the cosmic ray mesons was put forward by Heitler and various co-workers (1943, 4, 5). All the calculations are based on the version of the meson theory proposed by Möller and Rosenfeld (1940). This theory was formulated so as to give the best possible agreement with nuclear data. The theory assumes the existence of both charged mesons and neutral mesons. Further, the meson field is supposed to consist of two components—(1) the pseudo-scalar field, containing mesons of spin 0 and an average life corresponding to that observed for the mesons in cosmic rays; and (2) the vector field, containing mesons of spin 1 with a short life of the order of 10^{-8} sec.

The application of the Möller-Rosenfeld theory to fast collisions was made possible by a procedure suggested simultaneously by A. H. Wilson (1941) and by Heitler (1941). The procedure introduces radiation damping as an essential feature of the theory.

Using the Möller-Rosenfeld theory and using the radiation damping method, cross-sections for various high energy collisions involving mesons were calculated.

Heitler and Peng (1944) worked out the cross-section for the emission of mesons in the collisions between two fast nucleons. Hamilton and Peng (1944) calculated a number of other processes, such as the photo-electric emission of mesons, etc.

The cross-sections obtained for the emission of mesons in the collision between fast nucleons cannot claim great accuracy, as they have been evaluated with the semi-classical Weizsäcker-Williams method. We shall not make use of the actual values of the theoretical cross-sections; we shall merely assume that the cross-sections are large, and that, therefore, the cross-sections of the various nucleons inside the same nucleus overlap.

A. *The height of production of the meson component.*

(i) The primaries of the meson component are assumed to be protons. This assumption is supported by the interpretation of the geomagnetic

effects (Johnson (1938)). The primaries are unlikely to contain neutrons. The assumption of a strong neutron component would not be compatible with the geomagnetic evidence; besides, the neutron is believed to be unstable with a half-life of the order of hours; thus neutrons from distant sources could not reach the earth.

(ii) The primary protons entering the atmosphere of the earth are expected to collide with neucleons inside atomic nuclei, and thus emit mesons. The cross-sections of the separate nucleons in one nucleus are supposed to overlap, and, therefore, it is expected that one incident proton gives rise to a small group of mesons when traversing a nucleus. Such groups of mesons appear as small penetrating showers. The shower of fig. 16 may be an example of such a process.

It is also seen that a primary splits up its energy, giving rise to several mesons in accordance with what one should expect from the analysis of the geomagnetic effects (compare page 14).

(iii) The total cross-section for a collision with a nucleus must be expected to be of the same order as the geometrical cross-section of the nucleus. Assuming for the geometrical cross-section of a nucleus of mass-number A,

$$\Phi(A) = \pi(0{\cdot}54\, e^2/m_e c^2)^2 A^{2/3} \quad \ldots\ (23)$$

(Heisenberg, 1937)

we find for air

$$\Phi(\text{air}) = 4{\cdot}5 \times 10^{-25}\,\text{cm}^2 \quad \ldots\ (24)$$

and the mean free path of nucleons in air corresponding to the cross-section (24) is about

$$R_{\text{air}} = 1/N\Phi(\text{air}) \sim 60\, g \text{ per cm}^2 \quad \ldots\ (25)$$

This value represents, of course, only an estimate of the order of magnitude. Similarly, we obtain for the mean free path in lead

$$R_{\text{Pb}} \sim 140\, g \text{ per cm}^2 \quad \ldots\ (26)$$

The bulk of the mesons is expected to be produced near the top of the atmosphere inside the mean free path of the primary nucleons. Thus, according to (25), the bulk of the mesons should be produced in the first 60 g. per cm.^{2} of the atmosphere. Such a height of production is compatible with the observed absorption anomalies and also with the experiments of Schein and his co-workers (1943).

B. *Interpretation of the local penetrating showers.*

(i) It was shown that the local penetrating showers are due to primaries with a mean free path of the order of 100 g. per cm.^{2} in lead. Protons and neutrons have, according to (26), a mean free path of this order;

therefore, it may be assumed that the local penetrating showers are due to the emission of mesons in the collision of nucleons with atomic nuclei.

The nucleons initiating the penetrating showers can be assumed to be the remnants of the primary proton component, which we suppose to have given rise to the hard component at greater heights.

The primaries of the local penetrating showers were found to contain both charged and neutral primaries. This is in accordance with what one should expect. The primary protons falling on the top of the atmosphere are likely to change into neutrons in the course of meson production and the neutrons will be reconverted into protons. Thus, at a sufficiently great depth, the beam of protons is expected to change into a beam of protons and neutrons in equilibrium.

(ii) The intensity of the nucleon component at sea-level can also be understood in terms of the theory of meson production, as we show in the following.

We assume provisionally that the primary nucleons are absorbed exponentially, the absorption coefficient being independent of the primary energy. This assumption is justified provided we assume that a primary nucleon is completely absorbed in its first close encounter with nucleus.

For simplicity, we may assume that all primaries are protons (the conclusions are only slightly modified if one assumes, for instance, that 1/10th of the primaries are protons). The rate of protons incident on the top of the atmosphere may thus be assumed to be

$$J_{\text{prim}} = 2{,}000 \text{ per cm}^2 \text{ per hour all directions of incidence} \quad \ldots\ldots \quad (27)$$

The vertical intensity of these particles at a depth x below the top of the atmosphere is therefore

$$J(x)\, d\Omega = \frac{J_{\text{prim}}\, d\Omega}{2\pi} e^{-x/R} \quad \ldots\ldots \quad (28)$$

where R is the mean free path of the nucleons.

Integrating over all directions of incidence we have

$$\int J(x)\, d\Omega = J_{\text{prim}} \int_0^{\pi/2} e^{-x/R\cos\theta} \sin\theta\, d\theta,$$

and for $x \gg R$, we can assume in good approximation

$$\int_0^{\pi/2} e^{-x/R\cos\theta} \sin\theta\, d\theta \backsim\backsim \frac{R}{x} e^{-x/R},$$

thus the effective solid angle appears to be

$$\Omega = \frac{2\pi R}{x} \quad \ldots\ldots \quad (29)$$

and therefore the total flow of primaries at the depth of x_0, corresponding to sea-level is given by

$$J_{\text{sea-level}} = J_{\text{prim}} \frac{R}{x_0} e^{-x_0/R} \quad \ldots\ (30)$$

We have thus the following equation

$$\log_e (J_{\text{prim}}/J_{\text{sea-level}}) = x_0/R + \log_e (x_0/R) \quad \ldots\ (31)$$

The intensity at sea-level is estimated from the rate of penetrating showers observed. About 0·3 showers per hour were observed with a collecting area of 1000 cm.^{2}. Thus we have

$$J_{\text{prim}} = 3 \times 10^{-4} \text{ per hour per cm}^2 \quad \ldots\ (32)$$

We obtain from (27), (31) and (32)

$$x/R = 13$$

or

$$R = 77 \text{ gram per cm.}^2 \quad \ldots\ (33)$$

This value is in good agreement with the estimated mean free path given in Equation (25).

If we were to assume that the rate of primary protons is only 1/10th of the rate of incident particles, we would find instead of (33)

$$R = 90\,g \text{ per cm}^2$$
$$\text{for } J_{\text{prim}} = 200 \text{ particles per hour per cm}^2 \quad \ldots\ (34)$$

The above value is still in agreement with the order of magnitude estimate (25).

We conclude that the rate of local showers can be accounted for in terms of primaries which have traversed the atmosphere without suffering any close collisions with atomic nuclei (compare Jánossy (1943)).

C. *The origin of the soft component.*

It was suggested by Hamilton, Heitler and Peng (1943) that the soft component is not of primary origin, but is due to the decay electrons of transverse mesons. It is expected that the primary nucleons give rise to at least as many short-lived transverse mesons as ordinary pseudo-scalar mesons. The transverse mesons would decay almost immediately, and, therefore, they would give rise to the soft component.

It is difficult to decide whether this hypothesis is the correct one. It would be most important to get direct experimental evidence as to the existence of transverse mesons.

It was shown by Heitler and co-workers that many of the features of the soft component can be accounted for in terms of transverse mesons. We want to point out two difficulties encountered by such a hypothesis. Firstly, the absence of an E–W–asymmetry at high altitudes indicates that the soft and hard components at high altitudes are of different origins.

The second difficulty arises in connection with the observation of extensive air showers. In the high energy region, the spectrum of the decay electrons can be shown to obey a power law

$$dw/w^{z+2}$$

where the meson spectrum is supposed to be given by dw/w^{z+1}. Thus, the decay electron spectrum decreases with increasing energy more rapidly than the meson spectrum. It can be shown by an order of magnitude consideration that the decay spectrum with exponent $z + 2$ contains a much smaller number of high energy electrons than would be required to account for the observed rate of extensive air showers.

We may note that neither of the above difficulties necessarily rules out the possibility of the greater part of the soft component being, after all, due to decay. The first difficulty might be overcome by assuming that the lack of EW asymmetry at high altitudes is not due to the lack of asymmetry of the primaries, but that the observed symmetry is due to scattering of the electrons and other similar effects, which tend to mask the asymmetry of the primaries.

The second difficulty, concerning the extensive air showers, might also be overcome. Firstly, though very probable, it is by no means certain that the extensive air showers are large electron cascades. Secondly, the observed extensive air showers, even if of electronic nature, might be due to a few energetic primary electrons, which may be incident in addition to the main primary beam of protons.

In our opinion, though there is no decisive difficulty *against* the hypothesis of a common origin of the bulks of the soft and hard components, the evidence as a whole seems to weigh against such a hypothesis. It seems on the whole more likely that the two components are independent of each other.

V. The Cascade Theory.

It was shown by Bhabha and Heitler (1937) and by Carlson and Oppenheimer (1937) that most cosmic ray showers can be accounted for in terms of cascades; that is, in terms of subsequent processes of collision radiation by electrons and pair production of photons.

The average number of electrons and photons produced by a primary electron or photon in a given layer can be obtained as the solution of a certain diffusion equation. In the following we review the methods of

solution of this equation. It may be pointed out that the solutions finally obtained are most convenient for numerical computation.

Units of length and energy.

The cross-sections for both pair-production and collision radiation are proportional to

$$G = \frac{4r_0^2 Z^2}{137}\log_e(183\,Z^{-1/3}) \qquad \ldots\ (35)$$

Z = atomic number, $r_0 = e^2/m_e c^2$.

It is convenient, therefore, to introduce as a unit of length the following quantity

$$t_0(Z) = 1/NG = \frac{137}{4r_0^2 Z^2 N \log(183 Z^{-1/3})} \qquad \ldots\ (36)$$

where N is the number of nuclei per c.c. if t_0 is to be expressed in cms. alternatively, N is the number of nuclei per gram if t_0 is to be expressed in grams per cm.^{2}. We note the following numerical values:

$$t_0(\text{air}) = 342\text{ m.},\quad t_0(\text{Pb}) = 0{\cdot}52\text{ cm.} \qquad \ldots\ (37)$$

Electrons lose energy both by radiation and by ionisation. The rate of loss of energy due to radiation increases for high energies proportional to the energy; the loss due to ionisation increases only slightly with energy. Thus, for low energies, ionisation loss is more important than radiation loss, while for high energies, the radiation loss is predominant. A critical energy $E_c(Z)$ can be introduced as a rough limit between the region where ionisation loss is important and the region where radiation loss is important.

It is found convenient to define as the critical energy the energy lost due to ionisation along one cascade unit.

Thus it is approximately given by

$$t_0\left(\frac{dE}{dt}\right)_{\text{ion}} = 1 \qquad \ldots\ (38)$$

for $E = E_c(Z)$.

The critical energy for air is 100 MEV; the critical energy in lead is 7 MEV.

In the following we shall write ζ for a thickness expressed in cascade units, and w for an energy expressed as a multiple of the critical energy. Thus we shall write

$$\zeta = t/t_0 \quad \text{and} \quad w = E/E_c \qquad \ldots\ (39)$$

The Diffusion Equation.

We write for the probability that an electron of energy w emits a photon of energy between w' and $w' + dw'$ along a path $d\zeta$

$$a(w, w')\, dw'\, d\zeta \qquad \ldots\ (40)$$

Similarly, we write for the probability that a photon of energy w is absorbed emitting a pair, the positive electron of the pair having an energy between w' and dw'.

$$b(w, w')\, dw'\, d\zeta \qquad \ldots\ (41)$$

The actual expressions for a and b were given by Bethe and Heitler (1934).

Assuming a cascade contains $N(w, \zeta)\, dw$ electrons and $P(w, \zeta)\, dw$ photons, with energies between w' and $w' + dw'$ at a depth ζ, we can work out with the help of (40) and (41) the average changes dN and dP taking place along an element $d\zeta$ of path. As a result of a short calculation, the following equations are obtained (we write β for the rate of loss of energy due to ionisation; in our units we have, of course, $\beta = 1$).

$$\frac{\partial N}{\partial \zeta} = -N(w, \zeta) \int_0^w a(w, w')\, dw' + \int_0^\infty N(w + w', \zeta)\, a(w + w', w')\, dw' + 2\int_0^\infty P(w + w', \zeta)\, b(w + w', w)\, dw' + \beta \frac{\partial N}{\partial w}$$

$$\frac{\partial P}{\partial \zeta} = -P(w, \zeta) \int_0^w b(w, w')\, dw' + \int_0^\infty N(w + w')\, a(w + w', w)\, dw \qquad \ldots\ (42)$$

Solution of the diffusion equations.

For sufficiently high energies, namely, if the following condition is fulfilled,

$$\frac{w(w - w')}{w'} \gg 137\, m_e c^2 Z^{1/3} \qquad \ldots\ (43)$$

the functions a and b depend only on the ratio w/w'. The physical significance of (43) is that the screening of the atomic electrons must be complete for the collision. (See e.g. Heitler, Quantum theory of radiation.) In the following we shall deal only with approximate solutions of the system in so far as we shall assume that the functions a and b are

homogeneous, even for small energies. Thus we shall disregard the condition of full screening.

It was observed by Landau and Rumer (1938), that the system (42) can be simplified considerably by introducing the Laplace transforms of the numbers N and P. One introduces thus the following new variables, depending on an arbitrary new parameter s.

$$q(s, \zeta) = \int_0^\infty w^{s-1} N(w, \zeta)\, dw; \qquad p(s, \zeta) = \int_0^\infty w^{s-1} P(w, \zeta)\, dw \quad \ldots\ (44)$$

Multiplying the equations (42) by w^{s-1} and integrating over w, one finds an expression of the following form

$$\frac{\partial q(s, \zeta)}{\partial \zeta} = -A(s)\, q(s, \zeta) + B(s)\, p(s, \zeta) + (s-1)\beta\, q(s-1, \zeta)$$
$$\frac{\partial p(s, \zeta)}{\partial \zeta} = C(s)\, q(s, \zeta) - D p(s, \zeta) \quad \ldots\ (45)$$

where the functions $A(s)$, $B(s)$, $C(s)$ and the constant D are certain integrals which have been evaluated by Rossi and Greisen (1941) and independently by Bhabha and Chakrabarty (1943). We note that the transition from (44) to (45) is made possible by the functions a and b being homogeneous.

The equations (45) can be regarded as the infinite number of dependent differential equations. Approximate solutions of this system of equations has been obtained by Tamm and Belenky (1939).

In the following we shall reproduce the method of Bhabha and Chakrabarty in dealing with the system (45).

Solutions neglecting ionisation loss.

As a first step of solving (45), we derive approximate solutions by neglecting the ionisation term in the first equation (45). We shall thus deal with the equation

$$\frac{\partial q_0}{\partial \zeta} = -A(s)\, q_0 + B(s)\, p_0$$
$$\frac{\partial p_0}{\partial \zeta} = C(s)\, q_0 - D p_0 \quad \ldots\ (46)$$

The solutions of this equation are expected to give a good approximation of the correct solution for high energies, as for high energies, the loss due to ionisation cannot be assumed to be important. Solutions of (46) were

given by Serber (1938), Snyder (1938), Iwanenko and Sokolow (1938), and others.

For a fixed value of s, (46) represents a differential equation with constant coefficients. The solution of (46) can thus be written

$$q_0(s, \zeta) = M(s)\, e^{-\lambda\zeta} + N(s)\, e^{-\mu\zeta}$$
$$p_0(s, \zeta) = \frac{CM}{D - \lambda}\, e^{-\lambda\zeta} - \frac{CN}{\mu - D}\, e^{-\mu\zeta} \qquad \ldots\ (47)$$

where $M(s)$ and $N(s)$ are constants of integration and λ and μ are the solutions of the following secular equation

$$\begin{vmatrix} \lambda - A(s) & B(s) \\ C(s) & \lambda - D \end{vmatrix} = 0 \qquad \ldots\ (48)$$

So as to fix the notation of the two solutions of (48), we shall always assume that

$$\lambda(s) > \mu(s), \qquad \ldots\ (48a)$$
provided λ, μ are real

The constants M and N have to be determined so as to satisfy the initial conditions. The most interesting initial condition is that of a single electron of energy w_0 starting off a cascade at $\zeta = 0$. We find for this condition from (44)

$$q_0(s, 0) = w_0^{s-1}, \quad p_0(s, 0) = 0 \qquad \ldots\ (49)$$

And we find from (49) and (46)

$$M(s) = \frac{D - \lambda}{\mu - \lambda}\, w_0^{s-1} \quad N(s) = \frac{\mu - D}{\mu - \lambda}\, w_0^{s-1} \qquad \ldots\ (50)$$

The Mellin transform.

(i) The actual solutions N_0 and P_0 can be obtained from q_0 and p_0 by means of the Mellin transformation. According to the theory of the Mellin transformation, we have

$$N_0(w, \zeta) = \frac{1}{2\pi i} \int_{s_0 - i\infty}^{s_0 + i\infty} w^{-s}\, q_0(s, \zeta)\, ds,$$
$$P_0(w, \zeta) = \frac{1}{2\pi i} \int_{s_0 - i\infty}^{s_0 + i\infty} w^{-s}\, p_0(s, \zeta)\, ds \qquad \ldots\ (51)$$

The integrations in (51) have to be carried out along lines parallel to the imaginary axis to the right of all singularities of the integrand. With the help of (46), (50) and (51), we obtain the following equation—

$$N_0(w, \zeta) = \frac{1}{2\pi i\, w_0} \int_{s_0 - i\infty}^{s_0 + i\infty} \left(\frac{w_0}{w}\right)^s \left\{\frac{D - \lambda}{\mu - \lambda}\, e^{-\lambda\zeta} + \frac{\mu - D}{\mu - \lambda}\, e^{-\mu\zeta}\right\} ds \quad \ldots\ (52)$$

$$P_0(w, \zeta) = \frac{1}{2\pi i\, w_0} \int_{s_0 - i\infty}^{s_0 + i\infty} \left(\frac{w_0}{w}\right)^s \frac{C}{\mu - \lambda} \left\{e^{-\lambda\zeta} - e^{-\mu\zeta}\right\} ds$$

(ii) The following expressions derived from (52) are of importance:

1. Integral spectra. The numbers of electrons with energies exceeding w is given by

$$\overline{N}_0(w, \zeta) = \int_w^\infty N_0(w', \zeta)\, dw' \quad \ldots\ (53)$$

With the help of (52) and (53), interchanging the order of integrations we find

$$\overline{N_0}(w, \zeta) = \frac{1}{2\pi i} \int_{s_0 - i\infty}^{s_0 + i\infty} \frac{1}{s - 1} \left(\frac{w_0}{w}\right)^{s-1} \left\{\frac{D - \lambda}{\mu - \lambda}\, e^{-\lambda\zeta} + \frac{\mu - D}{\mu - \lambda}\, e^{-\mu\zeta}\right\} ds \qquad s_0 > 1$$

$\ldots\ (54)$

2. Spectrum of electrons produced by an incident power spectrum. Assume for the incident spectrum of electrons

$$s(w_0)\, dw_0 \begin{cases} = dw_0/w_0^{\gamma+1} & w_0 > w_1 \\ = 0 & w_0 \leqslant w_1 \end{cases} \quad \ldots\ (55)$$

We find for the number of electrons with energies exceeding w (with $w > w_1$) from (54)

$$S(w, \zeta) \equiv \int_w^\infty s(w_0)\, \overline{N}(w, \zeta)\, dw_0 =$$

$$\frac{1}{w_1^\gamma} \frac{1}{2\pi i} \int_{s_0 - i\infty}^{s_0 + i\infty} \frac{1}{(\gamma + 1 - s)(s - 1)} \left(\frac{w_0}{w}\right)^{s-1} \left\{\frac{D - \lambda}{\mu - \lambda}\, e^{-\lambda\zeta} + \frac{\mu - D}{\mu - \lambda}\, e^{-\mu\zeta}\right\} ds \qquad \gamma + 1 > s_0 > 1$$

$\ldots\ (56)$

The integral (56) can be evaluated by the method of residua. The path of integration can, namely, be deformed into a close path round the point $s = \gamma + 1$ we find eventually

$$S(w, \zeta) = \frac{1}{\gamma} \frac{1}{w^\gamma} \left\{ \frac{D - \lambda}{\mu - \lambda} e^{-\lambda\zeta} + \frac{\mu - D}{\mu - \lambda} e^{-\mu\zeta} \right\}_{s_0 = \gamma + 1} \quad w > w_1 \quad \ldots . \quad (57)$$

We see from (57) that an incident power spectrum produces a similar spectrum at any depth.

(iii) A number of useful expressions can be obtained considering the Laplace transforms of the various expressions with respect to ζ. (Compare Rossi and Greisen (1941), Nordheim and Hebb (1939)).

We introduce, for instance,

$$L_u(N_0) = \int_0^\infty e^{-u\zeta} N_0(w, \zeta)\, d\zeta \quad \ldots . \quad (58)$$

and with the help of (54) we find

$$L_u(N_0) = \frac{1}{2\pi i w_0} \int_{s_0 - i\infty}^{s_0 + i\infty} \left(\frac{w_0}{w}\right)^s \frac{D + u}{(\lambda + u)(\mu + u)}\, ds \quad \ldots . \quad (59)$$

It can be shown that for $s = 2$ we have $\lambda = 0$. Thus for $u = 0$, the integrand of (59) has a pole at $s = 2$. The integrand has further poles for larger values of s, but provided $w_0 \ll w$, the pole at $s = 2$ gives the most important contribution to the integral (59). Neglecting the contributions of the poles $s > 2$, one finds by the residuum method

$$L_{u=0}(N_0) \equiv \int_0^\infty N_0(w, \zeta)\, d\zeta = \frac{w_0}{w^2} \left(\frac{D}{\mu}\right)_{s=2} = 0{\cdot}437\, \frac{w_0}{w^2} \quad \ldots . \quad (60)$$

The last expression was obtained by introducing numerical values for D and μ.

Other useful expressions are obtained by evaluating derivatives of L_u with respect to u. A collection of the most important formulae thus obtained is given by Rossi and Greisen (1941).

Numerical evaluation of the Mellin integrals.

An integral of the type

$$J = \int_{-\infty}^{+\infty} e^{-\psi(x)}\, dx \quad \ldots . \quad (61)$$

can be evaluated by the saddle point method, provided the integrand has a pronounced maximum and decreases strongly to both sides of the maximum. Suppose, for example, that the function $\psi(x)$ has a minimum for $x = x_0$. Then we have

$$\psi'(x_0) = 0$$

and

$$\psi(x) = \psi(x_0) + (x - x_0)^2 \psi''(x_0)/2 + \text{terms of higher order.}$$

Neglecting terms of the third order, we have thus

$$J \sim e^{-\psi(x_0)} \int_{-\infty}^{+\infty} e^{-(x - x_0)^2 \psi''(x_0)/2}\, dx = \sqrt{2\pi}\, \frac{e^{-\psi(x_0)}}{\sqrt{\psi''(x_0)}} \quad \ldots . \quad (62)$$

The solutions of the cascade problem are represented by integrals of the type (52), thus of the type

$$J^* = \frac{1}{2\pi i} \int_{s_0 - i\infty}^{s_0 + i\infty} e^{-\psi(s)}\, ds \quad \ldots . \quad (63)$$

The integration has to be carried out along a line parallel to the imaginary axis. The intersections of the line of integration with the real axis has to be taken sufficiently to the right of the imaginary axis, but otherwise s_0 can be chosen arbitrarily. In particular, s_0 can be chosen so as to make

$$\psi'(s_0) = 0.$$

With this choice of s_0 we find for the value of the integral (63) according to (62)

$$J^* \sim \frac{e^{-\psi(s_0)}}{\sqrt{-2\pi\psi''(s_0)}} \quad \ldots . \quad (64)$$

provided $\psi''(s_0) < 0$.

(ii) From Equation (52), we find $N_0(w, \zeta) = J^*$ with

$$\psi(s) = -s \log_e \frac{w_0}{w} + \log \left\{ \frac{D - \lambda}{\mu - \lambda} e^{-\lambda\zeta} + \frac{\mu - D}{\mu - \lambda} e^{-\mu\zeta} \right\} \quad \ldots . \quad (65)$$

and therefore the value of s_0 can be determined from the following equation

$$\log_e \frac{w_0}{w} + \frac{d}{ds} \log \left\{ \frac{D - \lambda}{\mu - \lambda} e^{-\lambda\zeta} + \frac{\mu - D}{\mu - \lambda} e^{-\mu\zeta} \right\}_{s = s_0} = 0 \quad \ldots . \quad (66)$$

The second derivative is finally given by

$$\psi''(s_0) = \frac{d^2}{ds^2}\left\{\frac{D-\lambda}{\mu-\lambda}e^{-\lambda\zeta} + \frac{\mu-D}{\mu-\lambda}e^{-\mu\zeta}\right\}_{s=s_0} \quad \ldots. \quad (67)$$

Thus $N_0(w, \zeta)$ can be evaluated approximately by introducing (65), (66) and (67) into (64).

(iii) The procedure of evaluating the Mellin integrals can be somewhat simplified for sufficiently large thicknesses ζ. If ζ is sufficiently large, we have

$$\lambda(s_0)\zeta \gg \mu(s_0)\zeta \quad \text{(compare 46}a\text{)} \quad \ldots. \quad (68)$$

and the term containing the exponential $e^{-\mu\zeta}$ can be neglected in the equations (65), (66) and (67). We find in this case the following simple sets of equations:

$$\log_e \frac{w_0}{w} - \lambda'(s_0)\zeta + \frac{d}{ds}\left(\log\frac{D-\lambda}{\mu-\lambda}\right)_{s=s_0} = 0 \quad \ldots. \quad (69)$$

$$\psi''(s_0) = -\lambda''(s_0) + \frac{d}{ds^2}\left(\log\frac{D-\lambda}{\mu-\lambda}\right)_{s=s_0} \quad \ldots. \quad (70)$$

$$N_0(w, \zeta) = \left(\frac{w_0}{w}\right)^{s_0}\left(\frac{D-\lambda}{\mu-\lambda}\right)_{s=s_0} e^{-\lambda(s_0)\zeta}\Big/\sqrt{-2\pi\psi''(s_0)} \quad \ldots. \quad (71)$$

For given values of ζ and w_0/w, s_0 can be determined from the condition (69) and N_0 can then be determined with the help of (70) and (71).

Tables of the numerical values of the functions—

$$\lambda(s), \lambda'(s), \lambda''(s); \mu(s); \log\frac{D-\lambda}{\mu-\lambda}, \left(\log\frac{D-\lambda}{\mu-\lambda}\right)', \left(\log\frac{D-\lambda}{\mu-\lambda}\right)''$$

have been computed by Rossi and Greisen and others.

(iv) For practical purposes a much simpler procedure can be adopted. Instead of solving the equation (69) for s_0, it is much more convenient to consider s_0 as an *independent variable*. Thus for a fixed value of s_0, w_0/w, ζ and $N_0(w, \zeta)$ can be obtained as functions of the independent parameter s_0; as the result of a simple calculation, one finds, for instance,

$$\zeta = a_1(s)\log_{10}\left(\frac{w_0}{w}\right) + C_1(s) \quad \ldots. \quad (72)$$

$$\log_{10} N_0(w, \zeta) = a_2(s)\log_{10}(w_0/w) + b(s) - \tfrac{1}{2}\log_{10}\left(\log_{10}\frac{w_0}{w} + c_2(s)\right)$$

where $a_1(s), \ldots.$ are simple combinations of the functions $\lambda_1, \frac{D-\lambda}{\mu-\lambda}$, and their derivatives.

For the case of the integral spectrum $\overline{N_0}(w, \zeta)$ (compare (54)), we have evaluated the various coefficients. We find

$$\log_{10}(w_0/w) = A_1(s)\,\zeta + B_1(s)$$
$$\log_{10}\overline{N_0}(w, \zeta) = A_2(s)\log_{10}(w_0/w) - B_2(s) - \tfrac{1}{2}\log_{10}\left(\log_{10}\frac{w_0}{w} + C_2(s)\right) \quad \ldots\ldots \quad (73)$$

The coefficients A_1, B_1, A_2, B_2, C_2 are collected in the following table :—

TABLE 1.

$y =$	1, 2	1, 4	1, 6	1, 8	2, 0	2, 2	2, 4	2, 6	2, 8	3, 0
$A_1(s)$	4,104	1,586	0,908	0 603	0,430	0,318	0,240	0,183	0,141	0,109
$B_1(s)$	2,151	1,151	0,852	0,726	0,673	0,653	0,647	0,646	0,642	0,633
$A_2(s)$	0,441	0,708	0,875	0,969	1,000	0,967	0,861	0,662	0,350	- 0,103
$B_2(s)$	1,084	1,073	1,065	1,056	1,042	1,004	0,926	0,793	0,591	0,312
$C_2(s)$	0,676	0,452	0,456	0,508	0,571	0,619	0,640	0,639	0,619	0,586

The curves, fig. 24, have been computed with the help of (73) and Table 1.

We note that for $s = 2$ the equations (72) and (73) are identical with the expressions given for the position of the cascade maximum by various authors.

Cascade theory with collision loss.

The solutions so far obtained are only valid for energies largely exceeding the critical energy. For lower energies, the effects of collision loss cannot be neglected.

To deal with the effects of collision loss, it was suggested by Arley (1938), that in a first approximation, one can neglect ionisation loss for energies above the critical energy and neglect the radiative collisions for energies below the critical energy. Cascade tables were computed by Arley on these lines.

Attempts to deal analytically with the effects of collision loss have been made by various authors. It was suggested that the solutions N_0, not involving collision loss, should be taken as a first approximation of the correct solution, and the full solution was assumed to be given by a power series

$$N = N_0 + \frac{\beta}{w_0} N_1 + \left(\frac{\beta}{w_0}\right)^2 N_2 + \ldots, \quad \ldots\ldots \quad (74)$$

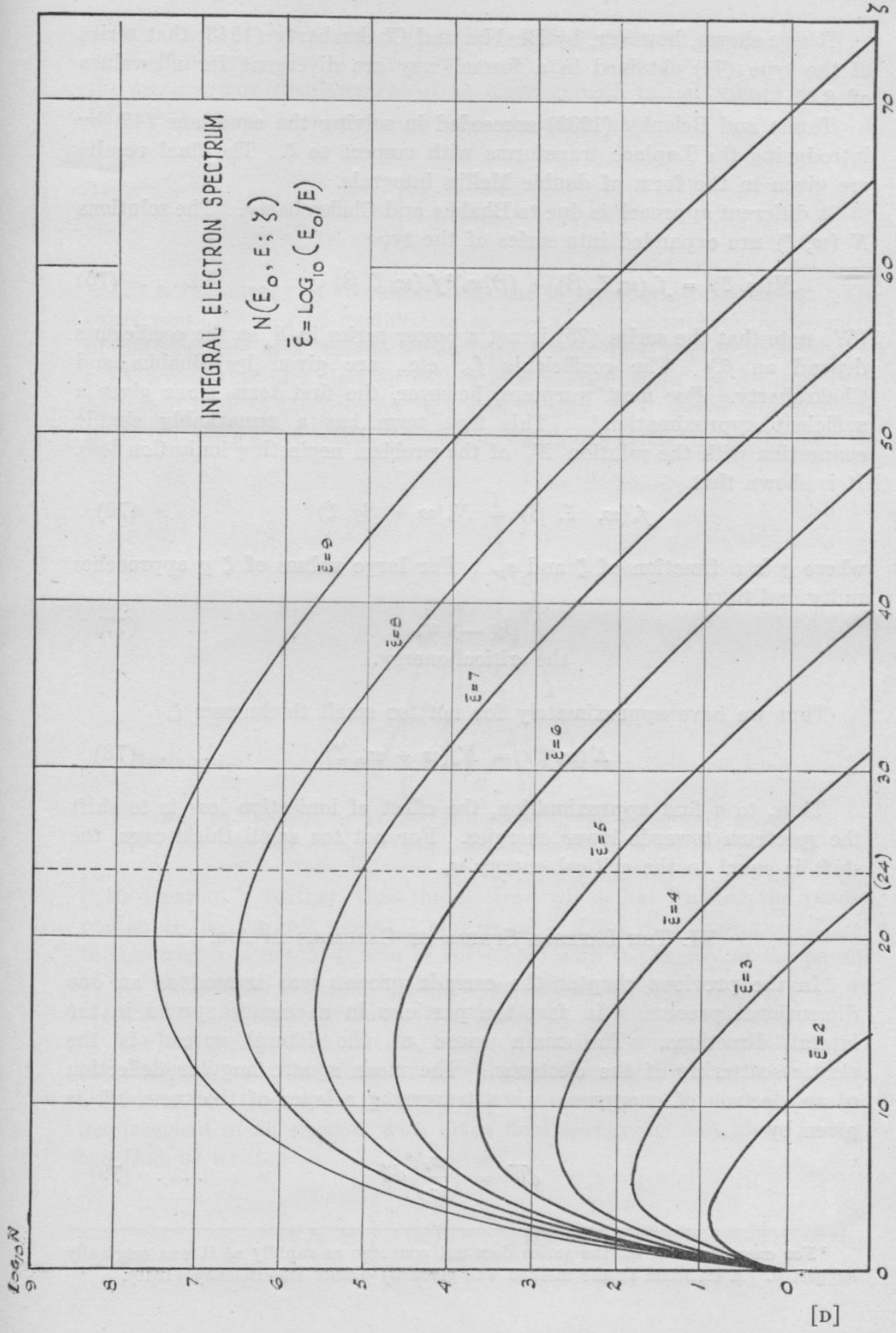

FIG. 24.—AVERAGE NUMBER OF ELECTRONS ($> E$) PRODUCED BY A PRIMARY (E_0) AS A FUNCTION OF DEPTH ζ

It was shown, however, by Bhabha and Chakrabarty (1943) that series of the type (74) obtained in a formal way are divergent for all values of β.

Tamm and Belenky (1939) succeeded in solving the equations (45) by introducing the Laplace transforms with respect to ζ. The final results are given in the form of double Mellin integrals.

A different approach is due to Bhabha and Chakrabarty. The solutions $N\ (w, \zeta)$ are expanded into series of the type

$$N(w, \zeta) = f_0(w, \zeta, \beta) + (\beta/w_0)^2 f_2(w, \zeta, \beta) + \ldots . \quad \ldots . \quad (75)$$

(We note that the series (75) is not a power series in β, as the coefficients depend on β.) The coefficients f_0, etc., are given by Bhabha and Chakrabarty. For most purposes, however, the first term alone gives a sufficient approximation.[7] This first term has a remarkably simple connection with the solution N_0 of the problem neglecting ionisation loss. It is shown that

$$f_0(w,\ \zeta,\ \beta) = N_0(w + \beta g, \zeta) \quad \ldots . \quad (76)$$

where g is a function of ζ and s_0. For large values of ζ g approaches unity and thus

$$\beta g \longrightarrow w_c \quad \ldots . \quad (77)$$

the critical energy.

Thus we have approximately for not too small thicknesses ζ,

$$N(w, \zeta) = N_0(w + w_c, \zeta) \quad \ldots . \quad (78)$$

Thus, to a first approximation, the effect of ionisation loss is to shift the spectrum towards lower energies. For not too small thicknesses, the shift is equal to the critical energy w_c.

VI. The Lateral Spread of Cascades in Air.

In the previous chapter the cascade process was treated as an one dimensional process. In fact the particles in a cascade spread in the lateral directions. The main cause of the lateral spread is the elastic scattering of the electrons. The mean square angular deflection of an electron of energy w when traversing a layer of thickness $d\zeta$ is given by

$$d\overline{\theta^2} = \left(\frac{w_s}{w}\right)^2 d\zeta \quad \ldots . \quad (79)$$

[7] For energies $w \ll w_0$ the series does not converge as rapidly as it was originally suggested. A criticism of the method was given by Tamm and Belenky (1946).

where $w_s = 21$ MEV, and ζ is measured in cascade units. As the result of a simple geometrical consideration we find with the help of (79) for the mean square displacement of an electron with initial energy w_0 after having traversed an absorber of thickness ζ.

$$\langle x^2 \rangle = \int_0^{\zeta} \left(\frac{w_0}{w(\zeta')} \right)^2 (\zeta - \zeta')^2 \, d\zeta' \qquad \ldots . \quad (80)$$

$w(\zeta')$ is the energy of the electron at the intermediate thickness ζ'. The expression (80) can be modified as to give the mean square displacement of the electrons in a cascade which have a fixed final energy w.

We note that any electron with a final energy w at the depth ζ' can be traced back to the primary in a unique way, as is shown schematically in fig. 25. We assume that the photon which has given rise to the electron

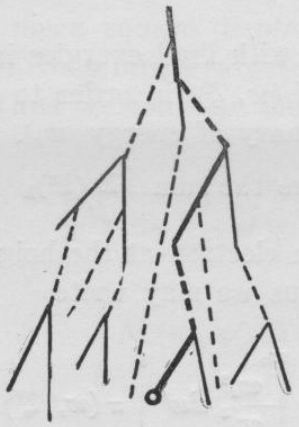

FIG. 25.—SCHEME OF A CASCADE SHOWER. (THE THICK LINE SHOWS HOW THE 'HISTORY OF A PARTICLE' CAN BE TRACED BACK TO THE PRIMARY).

is its "parent"; further, that the electron which has emitted the parent photon is the "grand parent," and so on. Thus, the energy $w(\zeta')$ of the electron to a depth ζ' can be correlated with the energy of the parent of the electron at that depth, the parent being the electron or photon on the trace of the final electron at the depth ζ', as shown in fig. 25.

The scattering of photons is, however, small as compared with that of the electrons, and, therefore, we can neglect the contributions to the total scattering by the parent photons of an electron. The mean square displacement of an electron with given final energy w and *given history* can thus be written

$$\langle x^2 \rangle_h = \int_0^{\zeta} a(\zeta') \left(\frac{w_s}{w(\zeta')} \right)^2 (\zeta - \zeta')^2 \, d\zeta' \qquad \ldots . \quad (81)$$

(the suffix 'h' denotes the 'history' of the electron), where

$$a(\zeta') = \begin{cases} 1 \text{ if the parent is an electron at } \zeta' \\ 0 \text{ if the parent is a photon at } \zeta' \end{cases} \quad \ldots\ldots \quad (82)$$

To get the mean square displacement of all electrons of final energy w it is necessary to average (81) over all possible histories which lead to the same final energy w at the depth ζ. This averaging can be carried out as follows.

We consider thus

$$\langle x^2 \rangle = \sum_h \langle x^2 \rangle_h / \delta \overline{N} \quad \ldots\ldots \quad (83)$$

where the sum has to be carried out over all possible histories leading to a final energy in the interval

$$w, \; w + dw \quad \text{and} \quad \delta \overline{N} = N(w_0, \; w; \; \zeta) \, dw$$

is the number of electrons with final energies in this interval. (We write $N(w_0, w, \zeta)$ instead of $N(w, \zeta)$ in order to emphasize that the cascade has been started by a primary of energy w_0).

We proceed to determine the sum $\sum_h \langle x^2 \rangle_h$

Note that the parent of an electron at the height ζ can have any energy between w and w_0. Thus we may write

$$\sum \langle x^2 \rangle_h = \int_w^{w_0} \frac{w_s^2}{w'^2} \, dw' \int_0^{\zeta} \pi(w,' \zeta') (\zeta - \zeta')^2 \, d\zeta'$$

where $\pi(w', \zeta') \, dw'$ is the number of parents in the energy interval $w', w' + dw'$ at the height ζ'. Parents which give rise to several final electrons in the interval $w, w + dw$ are counted several times, while photons are not counted at all.

The number of electrons at ζ' with energies in the interval $w', w' + dw'$ is given by

$$N(w_0, w', \zeta') \, dw',$$

each of these electrons starts a cascade and gives rise at the depth ζ to

$$N(w', w, \zeta - \zeta') \, dw,$$

final electrons in the interval $w, w + dw$. Thus the number of parents in the interval dw' is given by

$$\pi(w', \zeta') \, dw' = N(w_0, w; \; \zeta') \, N(w', w; \; \zeta - \zeta') \, dw' \, dw,$$

and, therefore, with the help of (83) and (84) we find for the mean square displacement

$$\langle x^2 \rangle = \frac{\int_0^{\zeta} \int_w^{w_0} \frac{w_s^2}{w'^2} N(w_0, w'; \zeta') N(w', w; \zeta - \zeta') (\zeta - \zeta)^2 \, dw' \, d\zeta' \quad \ldots . \quad (85)}{N(w_0, w, \zeta)}$$

Equation (85) was given by Bethe and by Nordheim (quoted from Rossi and Greisen).

Evalution of the mean square displacement of electrons in a cascade.

We evaluate the integral (85) using as a first approximation the approximate expression $N_0(w_0, w, \zeta)$ neglecting ionisation loss.

Further, it can be seen easily that the mean square displacement of an electron is mainly determined by the scattering in the last few cascade units. For large thicknesses, the mean square displacement cannot be assumed to depend on ζ. We shall, therefore, evaluate the mean square displacement averaged over ζ. Thus we consider the quantity

$$\langle\langle x^2 \rangle\rangle = \frac{\int_0^{\infty} N_0(w_0, w', \zeta) \langle x^2 \rangle \, d\zeta}{\int_0^{\infty} N_0(w_0, w', \zeta) \, d\zeta} \quad \ldots . \quad (86)$$

Introducing a new variable $\zeta - \zeta' = \zeta''$ we obtain with the help of (85) and (86)

$$\langle\langle x^2 \rangle\rangle = \int_w^{w_0} \frac{w_s^2}{w'^2} dw' \int_0^{\infty} N_0(w_0, w', \zeta') \, d\zeta' \int_0^{\infty} N_0(w', w, \zeta'') \, \zeta''^2 \, d\zeta'' \Big/ \int_0^{\infty} N_0(w_0, w; \zeta) \, d\zeta \quad \ldots . \quad (87)$$

The integrations with respect to ζ and ζ' can be evaluated approximately by means of (60). We find

$$\langle\langle x^2 \rangle\rangle = w_s^2 w^2 \int_w^{w_0} \frac{dw'}{w'^4} \int_0^{\infty} N_0(w', w, \zeta'') \, \zeta''^2 \, d\zeta \quad \ldots . \quad (88)$$

Replacing the upper limit w_0 of (88) by infinity, we obtain further with the help of (52)

$$\langle\langle x^2\rangle\rangle = (w_s/w)^2 \int_0^\infty \zeta''^2\, d\zeta'' \frac{1}{2\pi i} \int_{s_0-i\infty}^{s_0+i\infty} \frac{1}{4-s} \left\{ \frac{D-\lambda}{\mu-\lambda} e^{-\lambda\zeta''} + \frac{\mu-D}{\mu-\lambda} e^{-\mu\zeta''} \right\} ds \quad \ldots\ldots (89)$$

The integral with respect to s can be evaluated by the residuum method; as the result of a short calculation we find

$$\langle\langle x^2\rangle\rangle = (w_s/w)^2 \left\{ \frac{2}{\lambda^3} \frac{D-\lambda}{\mu-\lambda} + \frac{2}{\mu^3} \frac{\mu-D}{\mu-\lambda} \right\}_{s=4} \quad \ldots\ldots (90)$$

Introducing numerical values we find finally

$$\langle\langle x^2\rangle\rangle = 0.72\,(w_s/w)^2 \text{ (cascade units)}^2 \quad \ldots\ldots (91)$$

Similar results have been given by various authors.

(ii) The equation (91) gives the mean square spread of particles of energy w. This expression is, however, only valid for final energies much larger than the critical energy. The spread of the low energy particles can be estimated roughly in the following way.

Neglecting radiative collisions for electrons below the critical energy, we obtain for the mean square displacement suffered by an electron whose energy is reduced from the critical value to zero

$$\langle x^2\rangle = \int_0^1 \frac{w_s^2}{w_0^2\,(1-\zeta')^2} (1-\zeta')^2\, d\zeta' = \frac{w_s^2}{w_0^2} \quad \ldots\ldots (92)$$

(compare (80)). From (92) it is seen that the order of magnitude of the root mean square scattering of the very low energy particles should be

$$w_s/w_c \text{ cascade units.}$$

It is, therefore, plausible to assume that the mean square scattering of the particles of energy w is given by

$$\langle\langle x^2\rangle\rangle = 0,\,72 \left(\frac{w_s}{w + a\,w_c} \right)^2 \quad \ldots\ldots (93)$$

where a is a constant not very different from 1.

In particular, assuming $a = 1$, simple expressions for the density distribution of the particles in an extensive air shower can be obtained.

We hope to deal with some aspects of the problem of the density distribution in large cascades and the interpretation of experimental data concerning extensive air showers in a future publication.

Figures 3, 4, 16, 17 and 18 are shown on plates inserted at the end of the book.

I am greatly indebted to Dr. J. G. Wilson for kind permission to reproduce Figures 3 and 4; and to Dr. W. E. Hazen for permission to reproduce Figure 17.

REFERENCES.

ANDERSON 1932 Science **76**, 238.
„ 1933 Phys. Rev. **43**, 491; **44**, 406.
„ and NEDERMEYER 1934 Int. Conf. Phys. (London) 171.
ARLEY 1938 Proc. Roy. Soc. **A. 168**, 519.
„ and HEITLER 1938 Nature **142**, 158.
AUGER and MAZE 1938 Compt. Rend. **207**, 228.
„ „ and GRIVET MEYER 1938 Compt. Rend. **206**, 1721.
„ „ and CHAMINADE 1942 Phys. Rev. **62**, 307.
BETHE and HEITLER 1934 Proc. Roy. Soc. **A. 146**, 83.
BHABHA and CHAKRABARTY 1943 Proc. Roy. Soc. **A. 181**, 267.
„ and HEITLER 1937 Proc. Roy. Soc. **A. 159**, 432.
BLACKETT 1937 P.R.S. **A. 159**, 1 and 19.
„ and OCCHIALINI 1933 Proc. Roy. Soc. **A. 139**, 699.
„ and WILSON 1937 Proc. Roy. Soc. **A. 160**, 304.
BOTHE and KOLHÖRSTER 1929 Zeitschr. Phys. **56**, 751.
BOWEN, MILLIKAN and NEHER 1937 Phys. Rev. **52**, 80.
„ „ „ 1938 Phys. Rev. **53**, 217.
BRADDICK and HENSBY 1939 Nature **144**, 1012.
CARMICHAEL and DYMOND 1939 Proc. Roy. Soc. **A. 171**, 321.
CLAY 1930 Amst. Proc. **33**, 711.
COCCONI, LOVERDO and TONGIORGI 1943 Nouvo Cim, **1**, 314.
COMPTON 1933 Phys. Rev. **43**, 387.
DUPERIER 1944 Terr. Magn. Atm. El. **49**, 1.
EPSTEIN 1938 Phys. Rev. **53**, 862.
FUSSEL. Quoted from Euler and Heisenberg, Erg. d. exakt. Naturw. **17**, 1938.
HAMILTON, HEITLER and PENG 1943 Phys. Rev. **64**, 78.
„ and PENG 1944 Proc. Ir. Ac. **49**, 197.
HEISENBERG 1937 Akad. Wiss. Leipz. **89**, 369.
HEITLER 1937 Proc. Roy. Soc. **A. 161**, 261.
„ 1941 Cambr. Phil. Soc. Proc. **37**, 291.
„ and PENG 1944 Proc. Ir. Ac. **49**, 101.
„ and WALSH 1945 Rev. Mod. Phys. **17**, 252.
IWANENKO and SOKOLOW 1938 Phys. Rev. **53**, 910.
JÁNOSSY 1937 Zeitschr. Phys. **104**, 430.
„ 1941 Proc. Roy. Soc. **A. 179**, 361.
„ 1943 Phys. Rev. **64**, 345.
„ and INGLEBY 1940 Nature **145**, 511.
„ McCUSKER and ROCHESTER 1941 Nature **148**, 660.
„ and LOCKETT 1941 Proc. Roy. Soc. **A. 178**, 52.

JÁNOSSY and ROCHESTER 1943a Proc. Roy. Soc. **A. 181**, 399.
„ „ 1943b Proc. Roy. Soc. **A. 182**, 180.
„ „ 1944 Proc. Roy. Soc. **A. 183**, 181.
„ and ROSSI 1940 Proc. Roy. Soc. **A. 175**, 88.
JOHNSON 1938 Rev. Mod. Phys. **10**, 193.
„ and BARRY 1939 Phys. Rev. **56**, 219.
KEMMER 1938a Proc. Roy. Soc. **A. 166**, 187.
„ 1938b Proc. Cambr. Soc. **34**, 354.
KOLHÖRSTER, MATHES and WEBER 1938 Nature **26**, 576.
KUNZE 1933 Zeitschr. Phys. **80**, 559; **83**, 1.
LANDAU and RUMER 1938 Proc. Roy. Soc. **A. 166**, 213.
MAZE 1941 These Paris.
MILLIKAN, NEHER and PICKERING 1943 Phys. Rev. **63**, 234.
MØLLER and ROSENFELD 1940 Kgl. Dansk. Vid. Sel. **17.**
NEDDERMEYER and ANDERSON 1938 Phys. Rev. **54**, 88.
NEHER and STEVER 1940 Phys. Rev. **58**, 766.
NERESON 1942 Phys. Rev. **61**, 111.
NORDHEIM 1938 Phys. Rev. **53**, 694.
„ 1939 Phys. Rev. **55**, 506.
„ and HEBB 1939 Phys. Rev. **56**, 494.
REGENER, V. H. 1943 Phys. Rev. **64**, 250, 252.
ROCHESTER 1946 Proc. Roy. Soc. **A.** 178, 469.
ROSSI 1931 Zeitschr. Phys. **68**, 64.
„ 1933 Zeitschr. Phys, **82**, 151.
„ and GREISEN 1941 Rev. Mod. Phys. **13**, 240.
„ HILBERRY and HOAG 1940 Phys. Rev. **57**, 461.
„ and NERESON 1942 Phys. Rev. **62**, 417.
„ „ 1943 Phys. Rev. **64**, 199.
„ and REGENER, V. H. 1940 Phys. Rev. **58**, 837.
SCHEIN, IONA and TABIN 1943 Phys. Rev. **64**, 253.
SERBER 1938 Phys. Rev. **54**, 317.
SKOBELZYN 1927 Zeitschr. Phys. **43**, 354.
„ 1929 Zeitschr. Phys. **54**, 686.
SNYDER 1938 Phys. Rev. **54**, 960.
STÖRMER 1930 Zeitschr. Phys. **1**, 237.
STREET, WOODWARD and STEVENSON 1935 Phys. Rev. **47**, 891.
TAMM and BELENKY 1946 Phys. Rev. **70**, 660.
„ „ „ 1939 Journ. Phys. U.S.S.R. **1**, 177.
TRUMPY 1943 Det. Dansk. Vid. Sel. **20**, Nr. 6.
VALLARTA 1937 Nature **139**, 839.
„ 1938 "On the theory of the allowed cone of cosmic radiation."
„ 1939 Rev. Mod. Phys. **11.**
WATHAGHIN, SANTOS and POMPEIA 1940 Phys. Rev. **57**, 61.
WILLIAMS, E. J. 1934 Phys. Rev. **45**, 729.
„ and ROBERTS 1940 Nature **145**, 102.
WILSON, A. H. 1941 Proc. Cambr. Soc. **37**, 301.
YUKAWA 1935 Proc. Phys. Math. Japan. **17**, 48.

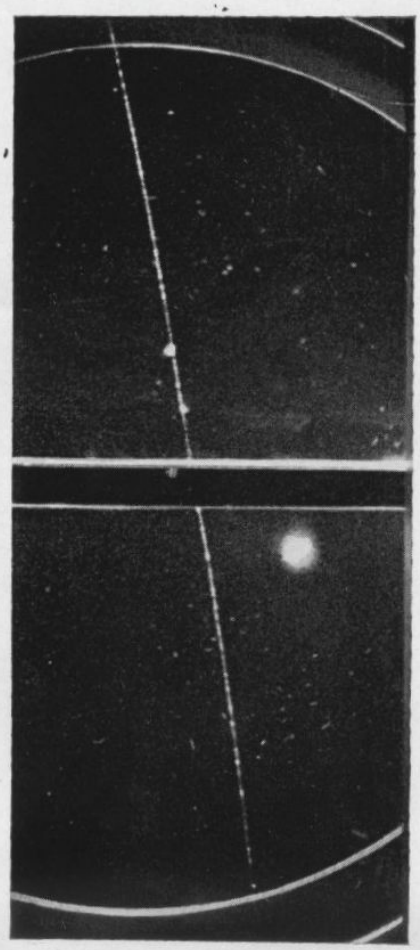

FIG. 3.—Penetrating particle
(J. G. Wilson).

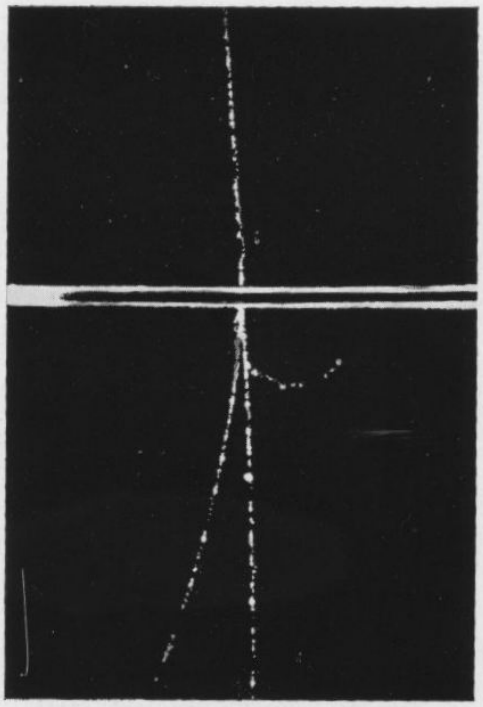

FIG. 4.—Electron.
(J. G. Wilson).

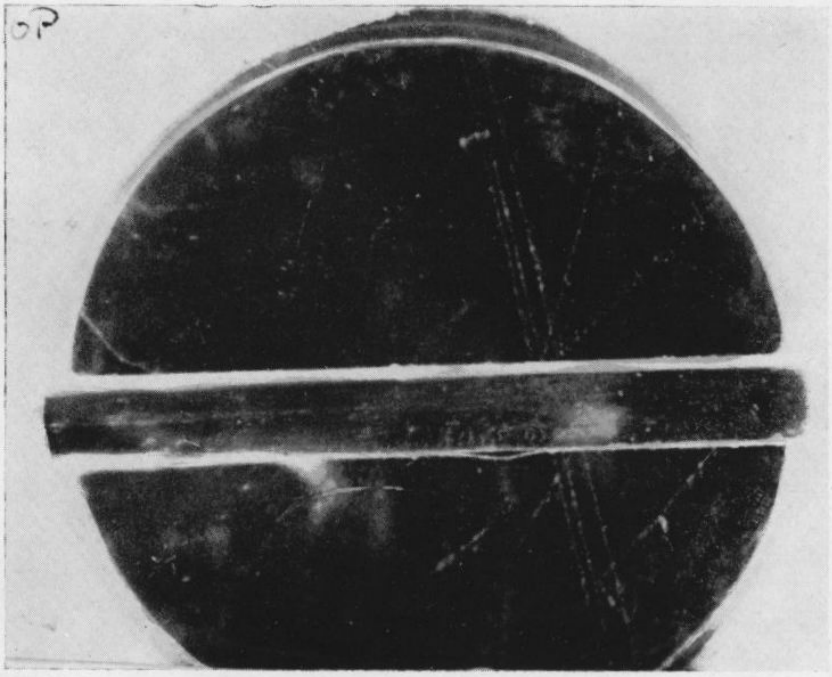

FIG. 16.—Penetrating shower (Jánossy, McCusker and Rochester).

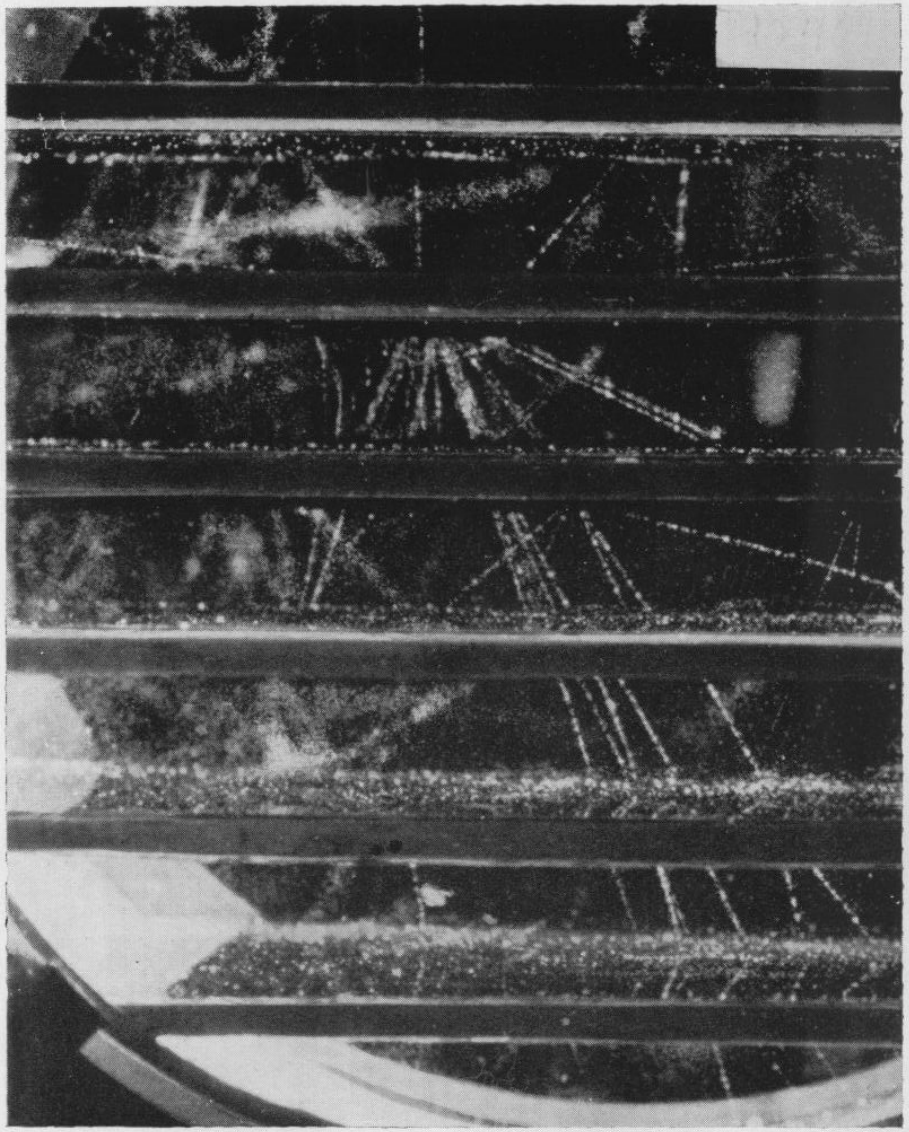

FIG. 17.—Penetrating shower (Hazen).

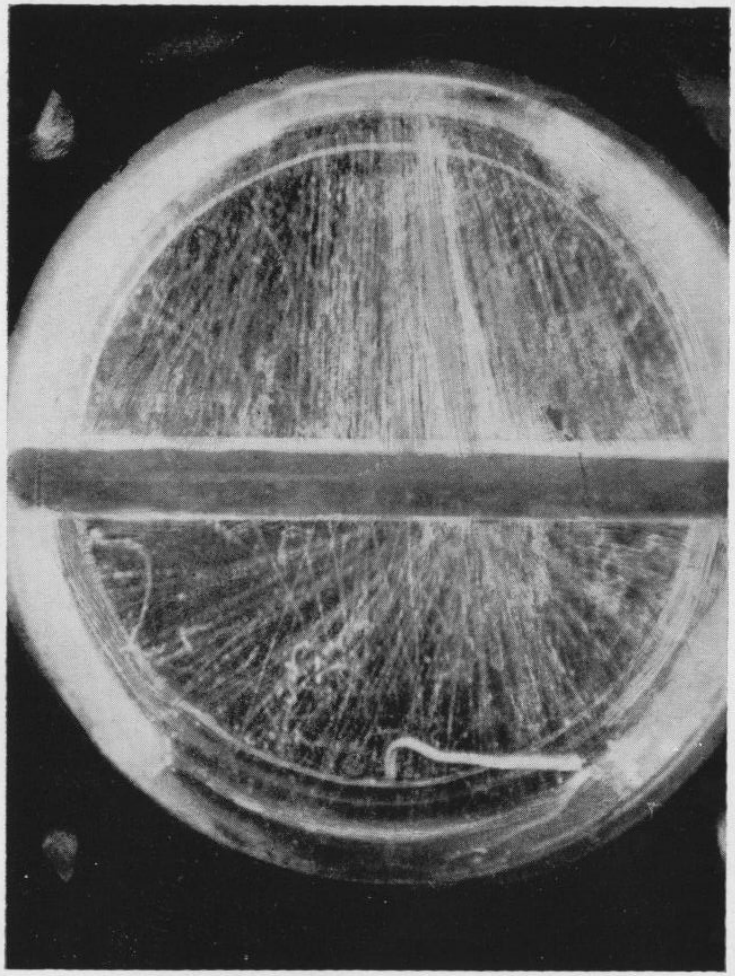

FIG. 18.—Penetrating shower (McCusker).